ISSN 1905-9094

GMSARN INTERNATIONAL JOURNAL

Vol. 3 No. 1
March 2009

Published by the

GREATER MEKONG SUBREGION ACADEMIC AND RESEARCH NETWORK
c/o Asian Institute of Technology
P.O. Box 4, Klong Luang, Pathumthani 12120, Thailand

GMSARN INTERNATIONAL JOURNAL

GMSARN MEMBERS

Asian Institute of Technology (AIT)	P.O. Box 4, Klong Luang, Pathumthani 12120, Thailand. www.ait.ac.th
Hanoi University of Technology (HUT)	No. 1, Daicoviet Street, Hanoi, Vietnam S.R. www.hut.edu.vn
Ho Chi Minh City University of Technology (HCMUT)	268 Ly Thuong Kiet Street, District 10, Ho Chi Minh City, Vietnam. www.hcmut.edu.vn
Institute of Technology of Cambodia (ITC)	BP 86 Blvd. Pochentong, Phnom Penh, Cambodia. www.itc.edu.kh
Khon Kaen University (KKU)	123 Mittraparb Road, Amphur Muang, Khon Kaen, Thailand. www.kku.ac.th
Kunming University of Science and Technology (KUST)	121 Street, Kunming P.O. 650093, Yunnan, China. www.kmust.edu.cn
National University of Laos (NUOL)	P.O. Box 3166, Vientiane Perfecture, Lao PDR. www.nuol.edu.la
Royal University of Phnom Penh (RUPP)	Russian Federation Blvd, PO Box 2640 Phnom Penh, Cambodia. www.rupp.edu.kh
Thammasat University (TU)	P.O. Box 22, Thamamasat Rangsit Post Office, Bangkok 12121, Thailand. www.tu.ac.th
Yangon Technological University (YTU)	Gyogone, Insein P.O. Yangon, Myanmar
Yunnan University	2 Cuihu Bei Road Kunming, 650091, Yunnan Province, China. www.ynu.edu.cn
Guangxi University	100, Daxue Road, Nanning, Guangxi, CHINA www.gxu.edu.cn

ASSOCIATE MEMBERS

Nakhon Phanom University	330 Apibanbuncha Road, Nai Muang Sub-District, Nakhon Phanom 48000, THAILAND www.npu.ac.th
Mekong River Commission	P.O. Box 6101, Unit 18 Ban Sithane Neua, Sikhottabong District, Vientiane 01000, LAO PDR www.mrcmekong.org
Ubon Rajathanee University	85 Sathollmark Rd. Warinchamrap UbonRatchathani 34190, THAILAND www.ubu.ac.th

GMSARN
INTERNATIONAL JOURNAL

GREATER MEKONG SUBREGION ACADEMIC AND RESEARCH NETWORK (http://www.gmsarn.org)

The Greater Mekong Subregion (GMS) consists of Cambodia, China (Yunnan & Guanxi Provinces), Laos, Myanmar, Thailand and Vietnam.

The Greater Mekong Subregion Academic and Research Network (GMSARN) was founded followed an agreement among the founding GMS country institutions signed on 26 January 2001, based on resolutions reached at the Greater Mekong Subregional Development Workshop held in Bangkok, Thailand, on 10 - 11 November 1999. GMSARN is composed of eleven of the region's top-ranking academic and research institutions. GMSARN carries out activities in the following areas: human resources development, joint research, and dissemination of information and intellectual assets generated in the GMS. GMSARN seeks to ensure that the holistic intellectual knowledge and assets generated, developed and maintained are shared by organizations within the region. Primary emphasis is placed on complementary linkages between technological and socio-economic development issues. Currently, GMSARN is sponsored by Royal Thai Government.

The GMSARN member institutions are the Asian Institute of Technology, Pathumthani, Thailand; The Institute of Technology of Cambodia, Phnom Penh, Cambodia; Kunming University of Science and Technology, Yunnan Province, China; National University of Laos, Vientiane, Laos PDR; Yangon Technological University, Yangon, Myanmar; Khon Kaen University, Khon Kaen Province, Thailand; Thammasat University, Bangkok, Thailand; Hanoi University of Technology, Hanoi, Vietnam; Ho Chi Minh City University of Technology, Ho Chi Minh City, Vietnam; The Royal University of Phnom Penh, Phnom Penh, Cambodia; Yunnan University, Yunnan Province and Guangxi University, Guangxi Province, China; and other associate members are Nakhon Phanom University, Nakon Phanom Province, Thailand; Mekong River Commission, Vientiane, Laos PDR and Ubon Rajathanee University, Ubon Ratchathani Province, Thailand.

GMSARN International Journal

Volume 3, Number 1, March 2009

CONTENTS

Power Quality Investigation of Grid Connected Wind Turbines

Trinh Trong Chuong

Abstract*— *With the continued expansion of the scale of wind power generation, the power quality problems due to grid connected wind farms are concerned widely. The voltage fluctuation and flicker and harmonics are main aspects of power quality problems. The fluctuation of wind farm output and grid voltage due to the random fluctuation of wind speed and inherent characteristics of Wind Turbines (WTs) may cause flicker severity. It is significant to investigate the impact of power quality on load and operation of power system. In this paper, the WTs instantaneously generated power and voltage at the point of common connection (PCC) with grid are simulated by considering all the aerodynamical and mechanical effects, which could affect them. The inherent effect of the wind speed on the entire blade swept area is simulated in the model of the wind speed. The generated power is obtained by the simulation of the wind speed time series into a WTs model. The flickermeter model which expresses voltage fluctuations is simulated according to the IEC standard 61000-4-15. The wind speed, WTs and flickermeter models are simulated in Matlab/Simulink software. Both of grid and site parameters, which affect voltage fluctuation, are investigated. These parameters have a wide influence on voltage fluctuation and flicker emission levels.

***Keywords*— Wind power generation, power network, power quality.**

1. INTRODUCTION

Wind turbine generators are increasingly becoming among the prominent components of power systems. Due to the stochastic nature of wind, electrical power delivered by this type of generation possesses similar features. Furthermore, WTs are usually integrated with the grid at remote terminals, far from central loads or conventional generation. This is raising certain reluctance on the part of utility companies to inject that source of power with unknown behavior and to evaluate the accompanied power quality considerations. Due to the importance of WT power quality considerations, standard IEC 61400-21 [1] provides procedures for determining the power quality characteristics of WTs.

The sources of fluctuations in the generated power are due to stochastic aspects that determine wind speed at different times and heights, and to deterministic or periodic effects. The largest periodic effect known as the tower shadow is at the frequency at which rotor blades pass by the tower. In the common three bladed horizontal axis WTs, this frequency is known as a 3p (p is the rotating frequency of the blade) frequency which is three times the rotational frequency [2]. The reactive power consumption of the WT asynchronous generator depends on the active generated power. The drawn reactive power increases with the increase of the generated active power. Therefore, the reactive power consumption of the generator fluctuates as the wind speed fluctuates. Due to the fluctuations in the active and reactive power, the voltage at PCC fluctuates.

Trinh Trong Chuong (corresponding author) is with Faculty of Electrical Engineering, Hanoi University of Industry, Cau Dien Road, Minh Khai Village, Tu Liem District, Hanoi, Vietnam. E-mail: chuonghtd@gmail.com.

Voltage fluctuation is a serious issue particularly for direct connected WTs because these turbines produce power dependent on the variations of the wind speed and inject it without conditioning into the grid. Voltage fluctuation disturbs the sensitive electric and electronic equipment. This may lead to a great reduction in the life span of most equipment [3]. The lighting flicker level is generally used to measure voltage fluctuation. A case studying the voltage level profile when the power system is integrated with wind generation is given [4]. The influence of WTs on consumer voltage quality is studied [5]. A frequency domain approach to WTs for flicker analysis is presented [6]. The need to accurately simulate the WTs and investigate their interaction with the grid is becoming so important, since the penetration of wind in certain areas reaches significant levels. A suggested nonlinear simulation depending on the collected measured data is presented [7]. This simulation employs the neural network technique to predict the WT output power. The modeling of WTs for power system studies is presented [8]. The aerodynamic loads of the WTs are represented and simulated in frequency domain [9]. A comprehensive model of mechanical part consists of a number of lumped inertias, elastically coupled to each other is presented [10], [11]. The problem in this model that it needs more manufacturer's design data about turbine elements which is not available in most cases. Soft tools and techniques used for modeling and design simulation of WTs are reviewed [12]. A simple approach to aggregated wind farm equivalent for the analysis of power system operation is presented [11].

This paper presents the comprehensive time-domain modeling of wind speed, WT and flickermeter and investigates the influence different factors on voltage fluctuation caused by WTs. The wind speed, WT and flickermeter models are implemented in Matlab/ Simulink. The wind speed produced from wind speed

model is applied to the aerodynamic model to extract the aerodynamic torque. This torque is fed to the drive train/generator models to simulate the electrical power from WT.

2. MECHANISM ANALYSIS

The impact of grid-connected wind farm on power quality depends on the following factors: WT type, wind farm layout, short circuit capacity of power network and power line parameters.

2.1 Schematic diagram of WT integrating into power network

In order to explain the mechanism of voltage fluctuation and flicker due to WT, fig 1 shows the schematic diagram of WT integrating into power network, where $\dot{E}$ represents the voltage phasor of WT terminal, $\dot{U}$ represents grid voltage phasor, R and X represent resistance and reactance of power line, respectively, and $\dot{I}$ represents the current.

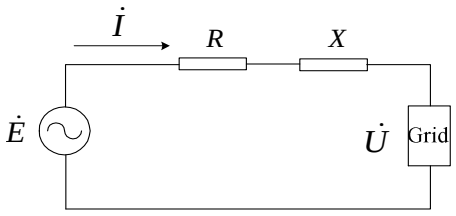

Fig. 1. Schematic diagram of WT integrating into power network.

It is assumed that the active and reactive output power are P and Q, respectively. So the following equation can be concluded.

$$\dot{U} = E - \frac{PR + QX}{E} - j\frac{PX - QR}{E} \quad (1)$$

Therefore, it can be seen that the grid voltage will fluctuate when the output power of WT is fluctuating, resulting in flicker. The mechanical power of WT can be represented by equation (2).

$$P = \frac{1}{2}\rho C_p(\lambda, \beta) A v^3 \quad (2)$$

here, P is power (W), ρ is air density(kg/m^3), A is swept area(m^2), v is wind speed(m/s), C_P is power coefficient, and λ is tip speed ratio:

$$\lambda = \frac{\omega R}{v} \quad (3)$$

here, ω is angular velocity of blade rotor (rad/s), and R is radius of blade rotor (m).

It can be seen from equation (2) that there are some factors causing output power of WT, such as air density, angular velocity of blade, pitch angle and wind speed and so on. The wind speed variation is stochastic, depending on meteorological condition. In general, it is not the main reason causing flicker because the frequency of wind speed variation is quite low. The variations of angular velocity of blade and pitch angle depend on WT type and control system. The variation of output power of WT can be decreased by the advanced control system.

2.2 Voltage fluctuation and flicker

During the WT continuous operation, the mechanical torque of WT is unstable due to wind shear, tower shadow effect and yawing uncertainty. The mechanical torque fluctuation will cause output power fluctuation. Generally, the frequency of output power fluctuation is same as frequency of blade rotor passing the tower. For WTs with three-blades, the frequencies of voltage fluctuations are 3p and times of 3p. As the frequency band of 3p is often in the range of 1~3Hz, the flicker severity produced by the periodic voltage fluctuations at these frequencies may be large part of the flicker severity.

The grid-connected WT not only cause voltage fluctuation and flicker during the continuous operation but also switching operation. The typical switching operation includes start-up and shutdown of WT and switching between generators (applicable only to WTs with more than one generator or a generator with multiple windings). These output power fluctuation due to switching operation will cause voltage fluctuation and flicker at the load node.

In this section we analyse the voltage variations produced when a source of variable power is connected to a weak network. We assume a simplified model representing the source of power (WT) and the grid impedance. The aim is to find an expression which gives the voltage at the generator terminal as a function of the power generated and the impedance of the grid (Fig. 2).

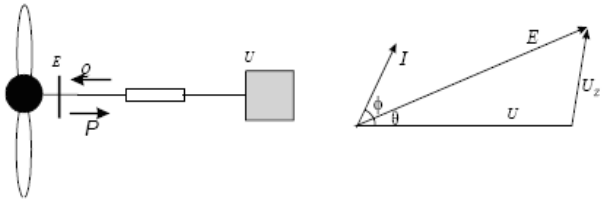

Fig. 2. Generator-grid model and phasor diagram.

From phasor diagram:

$$U_z^2 = U^2 + E^2 - 2EU\cos\theta = I^2(R^2 + X^2) \quad (4)$$

If $I^2E^2 = P^2 + Q^2$ we have:

$$\frac{P^2 + Q^2}{E^2}(R^2 + X^2) = U^2 + E^2 - 2.U.E.\cos\theta \quad (5)$$

From the phasor diagram:

$$E = U\cos\theta + RI\cos\phi - XI\sin\phi \quad (6)$$

After some manipulation:

$$E^4 - \left[2(PR - QX) + U^2\right]E^2 + \\ + (P^2 + Q^2)(R^2 + X^2) = 0 \quad (7)$$

Solving Equation above, the voltage E can be expressed as:

$$E = \sqrt{c_1 + \sqrt{c_1^2 - c_2}} \quad (8)$$

with:

$$c_1 = \frac{U^2}{2} + (PR - QX);\ c_2 = (P^2 + Q^2)(R^2 + X^2)$$

If we set Z equal to 0.05 p.u., and a constant voltage U= 1 p.u., the short circuit ratio is 1/Z = 20 for P=1 p.u. The power factor has been chosen equal to 0.97. Fig 3 shows the relation between E and the output power with the ratio X/R as a parameter for two different short circuit ratio SCR=20. The figures below show how the voltage varies with respect to the active power flow and the network characteristics [1].

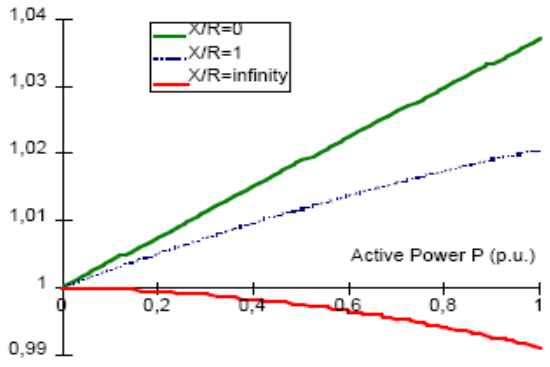

Fig 3. Voltage E as a function of active power, X/R.

The WT induction generator injects fluctuated active power into the grid and correspondingly it draws fluctuated reactive power from the grid. If the variation of the active power injected to the grid is ΔP and the corresponding variation of the reactive power absorbed from the grid is ΔQ, then voltage fluctuation, at PCC, ΔE/E, is given in (9). The nominal voltage is 1 pu. This can be rewritten as follows:

$$\frac{\Delta E}{E} = \Delta P.R - \Delta Q.X \approx \Delta S.Z\cos(\theta + \phi) \quad (9)$$

where:

- R resistance of the grid impedance (pu);
- X reactance of the grid impedance (pu);
- ΔS apparent power variation,

$$\Delta S = (\Delta P^2 + \Delta Q^2)^{1/2} \text{ (pu)};$$

- Z grid impedance amplitude (pu);
- θ grid impeadance angle; and φ is $\tan^{-1}(\Delta Q/\Delta P)$.

2.3 Harmonics

Harmonic distortion is another power quality problem due to wind power generation. For any type of WTs, harmonic current caused by generator can be ignored. The power electronic converter is real source of harmonic current. The constant speed WT will not produce harmonic current during the continuous operation, because there is not power electronic converter involved in WT. It will produce a little harmonic current when starting up, because soft-starter is in operation. But the start-up time is very short, the harmonic current due to start-up can be ignored.

However, a WT with power electronic converter will produce harmonic current, because the converter is always working during the continuous operation. In the normal operation, harmonics caused by WT depends on structure design of converter and filters installed in the WT, and also network short circuit capacity. Because the switching frequency of converter is not fixed, WT with force commutated converter will produce harmonic current as well as inter-harmonic current. The PWM switching converter and appropriate filters can minimize the harmonic distortion.

3. SIMULATION RESULTS

The studied model represents an equivalent of a distribution segment in LySon, VietNam. The model represents a 540kW wind power station consisting 3 turbines with Fixed Speed Induction Generator connected to the grid. Extend one of the 22kV lines to the WTs. The turbines are stall regulated types, with a rating of 180 kW each. The diesel generator power station has, at present, a very limited capacity of 850kW connected WTs.

The applicability of results from the simulation modelling depends how accurate and comprehensive the input data are that are used to build the model. Data collection was mostly carried out by the Institute of Energy, Vietnam.The main data groups for the model are:

- Power system circuit diagram
- Diesel generator specifications
- System controllers / operation procedures
- Power system transformers; Cables / overhead lines
- Loads and load profiles
- Other equipment e.g. storage, dump loads, etc.
- Wind resource

The data can be found in [11].

3.1 Samples of Results of Wind Speed and WT Modeling

Using the parameters of the WT generator which are given in the appendix, the wind speed and WT models have been implemented under Matlab/Simulink. The WT ratings are taken as base quantities. The grid fault level and X/R ratio are assumed 50 pu and 10 respectively. The no-load reactive power demand of the induction generator under study is compensated by capacitor banks

installed at PCC. Figure 4 presents a sample of selected model outputs; equivalent wind speed, active/reactive power and voltage at PCC.

The wind speed variation, assuming turbulence intensity of 10%, and v = 12 m/sec., is shown in Fig. 4(a). The corresponding aerodynamic power and electrical output power are shown in Fig. 4(b). Not all variations in the aerodynamic power are transmitted to the electrical power. It means that the soft shaft coupling and the inertia of WT rotor and generator rotor masses damp and smooth the variations of the aerodynamic power. Figure 4(c) shows the variation of the absorbed reactive power from grid. It is clear that the voltage fluctuation, in Fig. 4(d), is very small due the high fault level of the grid.

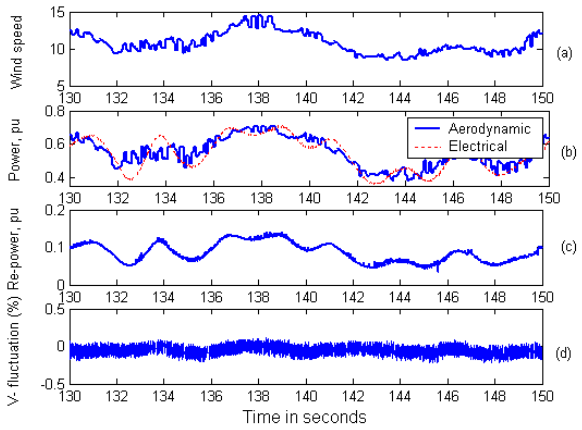

Fig. 4. Samples of the discussed modeling outputs (a) wind speed in m/sec. (b)- aerodynamic and electrical output power in pu (c)-absorbed reactive power in pu. (d)- voltage fluctuation at PCC (ΔE/E, %).

Figure 5 traces the variation of the absorbed reactive power with the injected active power for the integrated wind energy system and the induction generator under study. The drawn reactive power increases with the increase of the generated active power. This relation is known as P-Q characteristic of the induction generator.

The grid parameters affecting the WT flicker emission are the fault level, and X/R ratio of the gird impedance.

Fault Level

Figure 6 shows the variation of the short-term flicker index with different grid fault levels. This simulation test is carried out with two cases of grid impedance angles; 45^0 and 70^0. The mean wind speed at hub level is manitained at 12m/s and site turbulence is 10%.

X/R Ratio of grid impedance

The X/R ratio of the gird impedance is studied in terms of the impedance angle, $\theta = \tan^{-1}(X/R)$. Figure 7 shows the variation of the short-term flicker index with the impedance angle. The fault level is maintained at 10 pu. The mean wind speed at hub level is 12 m/sec. and site turbulence is 10%.

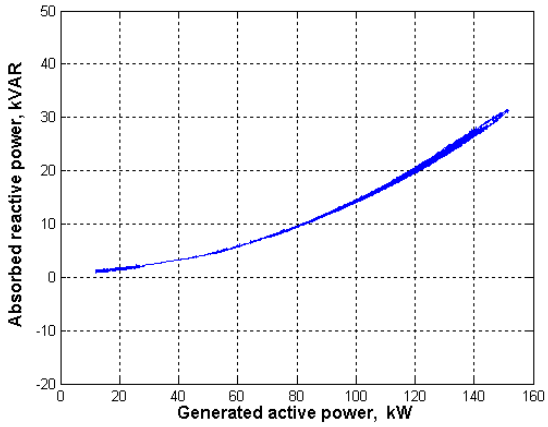

Fig. 5. The absorbed reactive power versus the injected active power for the induction generator under study.

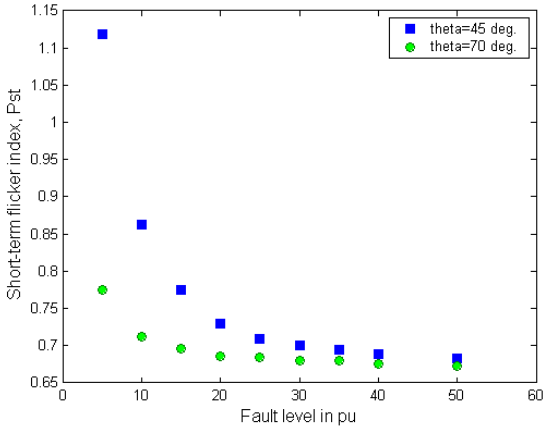

Fig. 6. Variation of P_{st} with the grid fault level.

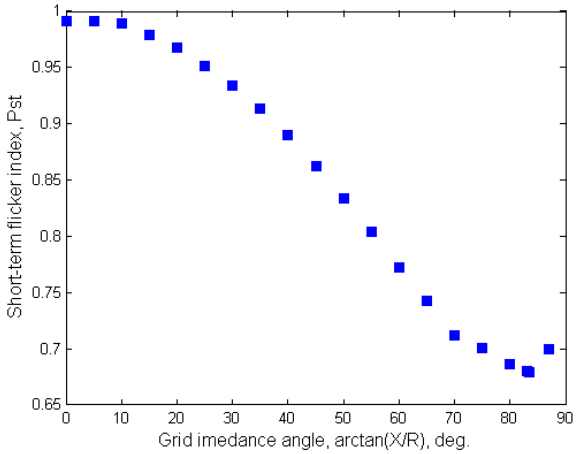

Fig. 7. Variation of P_{st} with the grid impedance angle.

3.2 Influences of Grid Parameters on Flicker Caused by WTs

From Fig. 7 it can be seen that the flicker decreases with the increase of until the minimum point, then the slope is reversed and flicker increases with increase of θ. The minimum point of voltage fluctuation is occurred when $\theta + \phi = 90^0$. The angle ϕ can be obtained according to the

incremental variation, ΔQ/ΔP, of P-Q characteristic of the induction generator (Fig. 5). The P-Q characteristic of the generator determines the ϕ-P relation.

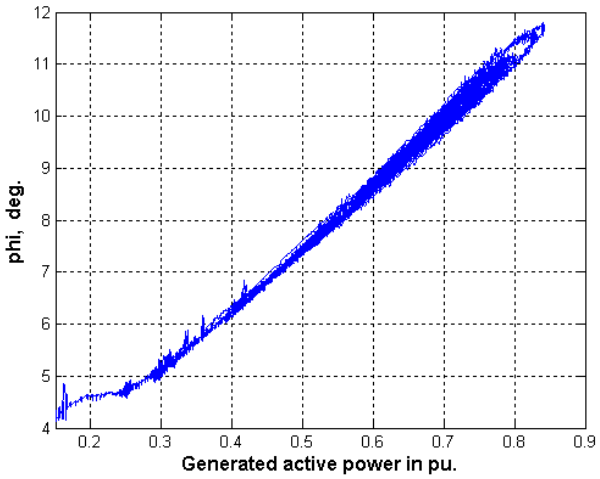

Fig. 8. Variation of the angle ϕ with generated active power for the induction generator under study.

Then the mean generated power (operating point) determines the value of φ and consequently $\theta = 90^0 - \phi$ at the point of minimum flicker emission. Figure 8 shows the variation of angle ϕ with the active generated power. The mean active generated power is estimated accordance to the WT power curve at mean wind speed. In this case, it is approximately 0.6 pu. as shown in Fig. 4(b). Then $\phi = 8.6^0$ which gives $\theta = 81.6^0$ at minimum flicker emission. The minimum point of flicker emission cannot be zero because the power swings up and down the mean value.

3.3 Effects of Site Parameters on WT Flicker Emission

Mean Wind Speed

The flicker severity is calculated for the same site turbulence (I_u=10%) and different mean wind speed. The fault level of the grid is 10 pu. The P_{st} values versus the mean wind speed are estimated for two grid impedance angles, 45^0 and 70^0.

The P_{st} variation with the mean wind speed is illustrated in Fig. 9. It can be explained by the WT power curve, shown in Fig.10. From Fig. 9, it can concluded that the output power and its fluctuations in the low wind region are low and therefore the induced voltage fluctuation is small. As the wind speed increases from cut in speed to 13 m/sec., the output power fluctuations and P_{st} increase, approximately in linear relation with the mean wind speed. However, in the stall region (greater than 13 m/sec.), the rate of change of the aerodynamic power curve is reduced, resulting in a corresponding reduction in the output electrical power variability. Then P_{st} values vary in small range with the increase of the wind speed as shown in Fig. 9.

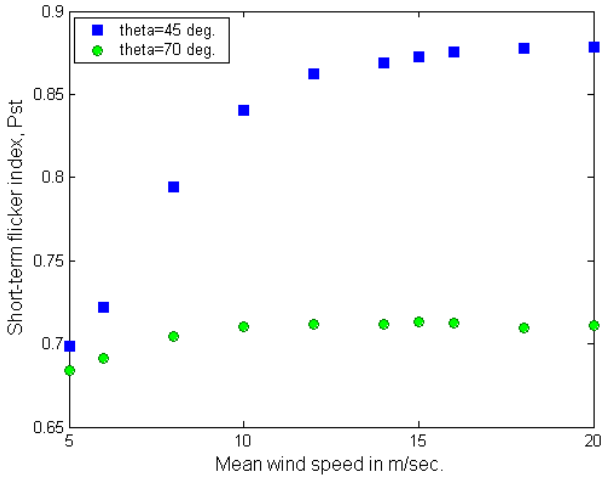

Fig. 9. Variation of P_{st} with mean wind speed for 45^0 and 70^0.

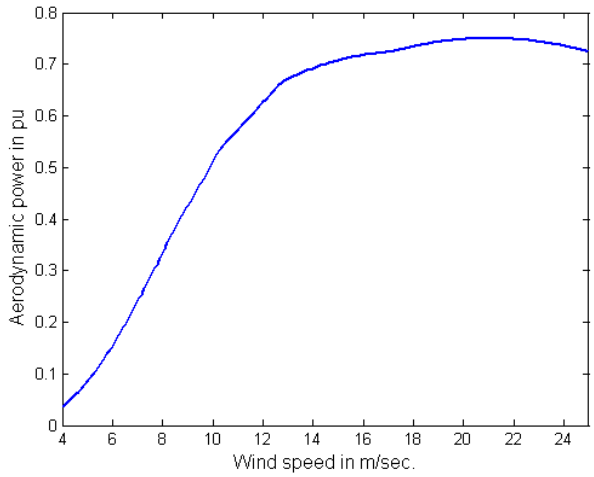

Fig. 10. WT power curve.

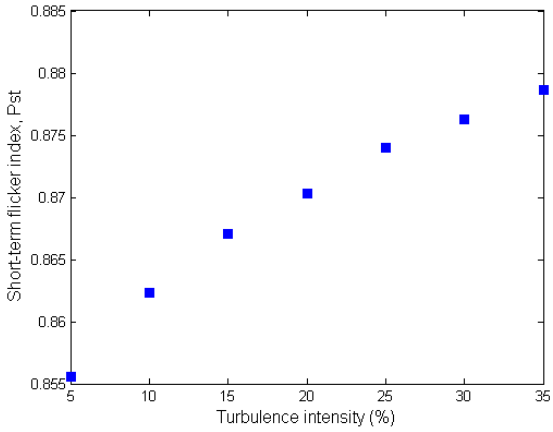

Fig. 11. Variation of P_{st} with wind speed turbulence.

Turbulence Intensity

In this case, the mean wind speed at hub level is maintained at 12 m/sec., the fault level is 10 pu., and the grid impedance angle is 45^0. Figure 11 shows the variation of P_{st} with the turbulence intensity. The

increase in the wind speed turbulence increases the power variability then the flicker emission increases with the increase of the turbulence intensity.

4. CONCLUSION

The comprehensive wind speed and WT models can be applied for voltage fluctuation and power quality studies. The flicker level caused by voltage fluctuation is evaluated by the flickermeter, described in IEC 61000-4-15. From simulation results, voltage fluctuations are widely affected by the grid strength and X/R ratio of grid internal impedance. The flicker emission is decreased with higher fault levels. The risk of voltage fluctuation increases in the resistive grids. The WT operating point and the Q-P characteristic of the generator determine the point of minimum flicker emission. The trend of flicker variation with the mean wind speed depends mainly on the WT power curve. The power variability and consequently flicker emission increases with turbulence increase. A wide look on the results indicates that grid parameters have more effect on flicker emission than site parameters.

REFERENCES

[1] IEC 61400-21. 2001. WT generator systems – Part 21: Measurement and assessment of power quality characteristics of grid connected WTs.

[2] Dolan, D. S. L. and Lehn, P. W. 2005. Real-time WT emulator suitable for power quality and dynamic control studies. In *Proceedings of the International Conference on Power Systems Transients*, Canada, June 19-23.

[3] Marei, M. I., El. Saadany, E.F. 2004. Estimation techniques for voltage flicker envelope tracking. *Electric Power System Research*, vol. 70, pp. 30–37.

[4] Trinh T. C. 2008. Voltage stability analysis of grid connected wind generators. *International Conference on Electrical Engineering*, Okinawa - Japan, 6-10 July.

[5] Tande, J. O. 2002. Applying power quality characteristics of WTs for assessing impact on voltage quality. *Wind Energy*, vol. 5, Issue 1, pp. 37-52.

[6] Vu V. T. 2006. Impact of distributed generation on power system operation and control. PhD thesis, Katholieke Universiteti Leuven, Leuven.

[7] Kelouwani, S. and Agbossou, K. 2004. Nonlinear model identification of WT with a neural network. *IEEE Trans. on Energy Conversion*, vol. 19, no. 3.

[8] Slootweg, J.G. 2003. Wind Power: Modelling and Impact on Power System Dynamics. PhD thesis, Delft.

[9] Søerensen, P. 1994. Frequency domain modeling of WTs structures. Risø-R-749 (EN).

[10] Soens, J., Vu V. T., Driesen, P., and Belmans, R. 2003. Modeling WT generators for power system simulations. *European Wind Energy Conference EWEC*, Madrid, 16 – 19 June.

[11] Trinh T. C. 2008. Effect of Voltage drop on dynamic respons of WT generator and recommanded setting level for under voltage protection. *Journal of Science and Technology*, No 63/2008, Vietnam.

[12] IEC 61000-4-15. 1997. Electromagnetic compatibility (EMC)-Part 4: Testing and measurements techniques -Section 15: Flickermeter, Functional and design specifications; 1st edition.

APPENDIX

The WT Data, Drive Train Data and Generator Data are stated as follows:

- Rated power 180 kW;
- Hub height 30 m;
- Rotor diameter 23.2 m;
- Number of blades three;
- Rotor speed 42 r/min;
- Blade profile NACA-63 200;
- Gearbox ratio 23.75.
- Turbine inertia 102.8 $kg.m^2$;
- Generator inertia 4.5 $kg.m^2$;
- Stiffness of the shaft 2700 N.m/rad;
- Nominal voltage 400 V;
- Number of pole-pairs three;
- Stator resistance 0.0092 Ohm;
- Rotor resistance (referred to the stator) 0.0061 Ohm;
- Stator leakage inductance 0.186 mH;
- Rotor leakage inductance (referred to the stator) 0.427 mH;
- Magnetizing inductance 6.7 mH.

Optimal Placement of PMU and RTU by Hybrid Genetic Algorithm and Simulated Annealing for Multiarea Power System State Estimation

Thawatch Kerdchuen and Weerakorn Ongsakul

Abstract*— *This paper proposes a hybrid genetic algorithm and simulated annealing (HGS) for solving optimal placement of PMU and RTU for multiarea power system state estimation. Each power system control area includes one PMU and several RTUs. Voltage magnitude, voltage angle, and real and reactive current are measured by PMU while the injection and flow of real and reactive power are measured and monitored through RTU. The power injection and flow measurement pairs are placed to observe the raw data of boundary bus and tie line for data exchange in wide-area state estimator. The critical measurement identification is used to consider the critical measurement free in each area. To reduce the number of measurements and RTUs, a PMU is placed at the bus with the highest number of connected branches. The power injection and flow measurement pairs and RTUs are optimally placed to minimize the installation cost of RTUs and power injection and flow measurement pairs. The results of 10-bus single area, IEEE 14 with 2 areas and 118-bus with 9 areas systems are the optimal measurement placement with critical measurement free. Comparison with simulated annealing (SA) is also made.

***Keywords*— Hybrid genetic algorithm and simulated annealing, Power system state estimation and Measurement placement.**

1. INTRODUCTION

Power injection and power flow measurement as well as RTU are commonly used in nowadays power system. Conventional power system state estimation uses the online power measurement pairs via RTU for providing the system data to state estimator at control centre. When the system becomes large or connected grids, multiarea power system state estimation should be used to estimate the wide-areas system states. PMU should be introduced into power system for increasing the accuracy of estimated system states. Thus, optimal PMU and RTU placement needs to consider for each area observability with low cost, also entire system states can be estimated by central state estimator.

Multiarea system state estimation by mixed measurements is introduced by many researchers [1-3]. Two levels state estimation are effectively used since the boundary measured data are exchanged [1]. First level, conventional state estimation is introduced to all areas. The voltage phase angle of each area and raw data of boundary buses are sent to the central control centre, then the second level state estimation is implemented for wide-area state estimation. This estimation makes the unbiased estimate for the entire system state [1, 2]. In contrast, the power system is decomposed and then the PMUs are installed to make the area observable [4]. Then, the entire system states of all areas are estimated by the centrally control centre. However, in [4], the tie line data are not observed and also bad data is not mention. More benefit of PMU in power system is voltage stability analysis [5]. The PMU is installed at the bus of each area with largest displacement of the voltage [5]. Similarly, PMU is also installed for a real-time voltage monitoring [6]. Many evolution algorithms are implemented to solve the measurement placement [7-8]. These algorithms are easily implemented and yield the good answers.

In this paper, the optimal placement of a single PMU and RTUs for each power system area by developed hybrid genetic algorithm and simulated annealing (HGS) is proposed. Each tie line is considered belonging to both this area and neighboring area to ensure that bad data can be identified in the central state estimator. The critical measurement [9] free of each area is considered for bad data detection. A PMU is installed at the bus with the highest incident lines. Number of several RTUs with power injection and flow measurement pairs is minimized by a HGS [7]. The advantage of HGS is the diversity of solution population can give the new search direction. Also, stochastic simulated annealing (SA) [8] is introduced to solve for the result comparison.

2. FUNDAMENTAL OF MEASUREMENT PLACEMENT FOR MULTIAREA STATE ESTIMATION

Area of power system might depend on topography. State estimator of each area estimates the local system states and other applications that gain by local estimated states may be introduced to that area. The central control centre collects the slack bus data of all areas, raw data at boundary buses and tie line, and then the wide-area system states are estimated.

For each area with PMU, the voltage magnitude and angle and real and reactive of current flow in the incident branches are measured, thus the linear model measurement Jacobian can be written as follows [10].

Thawatch Kerdchuen (corresponding author) is with Rajamangala University of Technology Isan, Nakhonratchasima, Thailand. E-mail: thawatch.ke@gmail.com.

Weerakorn Ongsakul is with the Energy Field of Study, Asian Institute of Technology, Thailand.

$$\mathbf{H}_{PMU} = \begin{array}{c} \\ \delta_i \\ \mathbf{I}_{ij} \\ \\ \end{array} \begin{array}{c} \begin{array}{cccc} \delta_i & \delta_j & & \end{array} \\ \begin{bmatrix} . & . & . & . \\ . & 1 & . & . \\ . & 1 & -1 & . \\ . & . & . & . \end{bmatrix} \end{array}$$

If we consider the bus with PMU as a slack bus, the column of δ_i will be deleted. Thus, if the conventional measurement pairs, power flow and injection measurement pairs, that connect via RTU, the entire linear model measurement Jacobian or measurement matrix $\mathbf{H}$ of each area is as follows

$$\mathbf{H} = \begin{bmatrix} \mathbf{H}_{PMU} \\ \mathbf{H}_{RTU} \end{bmatrix} \quad (1)$$

The $P\delta$ observability analysis can be introduced. The measurement system is observable if $rank(\mathbf{H}) = n-1$, where n is number of area system buses. Bad data in measurement of each area can be detected if the measurement system is without critical measurement. Critical measurement (*cm*) can be easily identified by residual analysis [11].

Area of power system for multi-area state estimation can be separated by using the tie line including. This including of tie line makes observable tie line since the measurement will be placed. Also, the areas are overlapping. The typical figure of this separated area is shown as follows

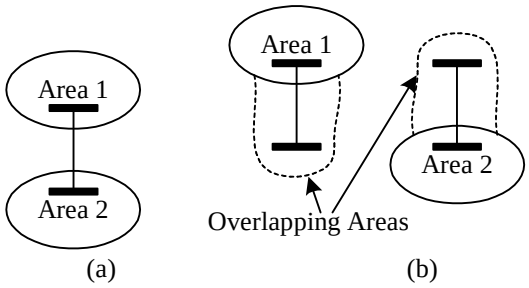

Fig. 1. Typical area separation (a) two areas system (b) area separation for measurement placement

Since the PMU can directly measure the phasor of system bus voltage, only one PMU per one area is sufficient for state estimation in the control center.

3. HGS IMPLEMENTATION FOR OPTIMAL PLACEMENT OF PMU AND RTU

A PMU is considered to place at the bus with maximum branch incident number. Then, HGS [7] is used to minimize the measurement pairs of power injection and flow and RTUs cost. Cost function uses only the conventional measurement cost, since the necessary PMU needs only one per one area. Thus, the remaining RTUs and measurement pairs cost can be formulated as follows

$$\text{Min} \quad Cost(z) = \sum_{i=1}^{R_T} (CR_i + \sum_{j=1}^{m_i} CM_{ij}) \quad (2)$$

subjects to the observability constraints

$$zero\_pivot = 1 \quad (3)$$

or

$$rank(\mathbf{H}) = N - 1 \quad (4)$$

where R_T is the number of RTUs, m_i is the number of measurement pairs (PQ) connected to i^{th} RTU, *CR* is the cost of RTU, *CM* is the cost of measurement pair. The matrix $\mathbf{H}$ in (4) is related with the terms of current flow measurement of PMU and power measurement pair installations. Constraint (3) is used when the triangular factorization or numerical method is used for observability analysis. In (3), zero pivot encounters during the factorization. Constraint (4) is used when the $P\delta$ observability concept used.

The solution cost evaluation is following to (2) with the penalties. Penalties include the observability and critical measurement. However, the minimum penalty part is observability result.

$$\text{Min} \quad Cost(z) = R_T \cdot CR + m_T \cdot CM + Penalties \quad (5)$$

$$\begin{aligned} Penalties &= Penalty1 + Penalty2 \\ Penalty1 &= \left[N - 1 - rank(\mathbf{H})\right](N \cdot N_L)^2 \\ Penalty2 &= (\text{No. of } cm)(N \cdot N_L) \end{aligned} \quad (6)$$

where N_L is the line numbers, m_T is the total number of measurement pairs, the measurement pair cost *CM* is 4.5 unit of currency and the RTU cost *CR* is 100 unit of currency [1, 2]. The first penalty is appeared if system is unobservable. The *penalty*2 is occurred if the system is with critical measurement.

In fitness evaluation of HGS [7], the measurement matrix $\mathbf{H}$ is formed for all chromosomes and all generations. The network observability is checked by the $P\delta$ observability analysis in all chromosomes. The measurement pair and RTU costs will converge to the minimum cost. The fitness function of HGS is according to the cost in (5) as follows.

$$fit = \frac{1}{1 + Cost(z)} \quad (7)$$

The fitness function of HGS is maximized of the inverse of measurement pair and RTU costs and penalty values. The cost plus one protects the divide by zero.

The process of optimal placements of PMU and RTU is start at the system area separation. This separation might be depended on the topography. However, in this paper the system areas are separated as in [1, 3]. The tie line is belonging to both areas. The overall process of optimal placement is as follows.

Step 1: The system is decomposed into each area. System tie line is defined as the radial line of

both areas that tie line incident. If the external bus has more than one line incident to same area, only one line is considered for area decomposition.

Step 2: Each area, the system bus with the first largest number of system line incident is selected for PMU placement. This system bus is chosen as the slack bus of area.

Step 3: HGS is introduced for optimal conventional measurement pair and RTU placement of each area.

Here, the current injection measurement [4] is also placed at PMU bus. This current injection measurement handles the critical measurement of current flow measurement in the incident branches, since any single measurement of a PMU can be lost while the branches are observable. This current injection measurement placement condition reduces the critical measurement identifying process of a PMU part.

For described HGS process, the process steps of HGS are explained as follows.

Step 1: Read the system topology of each area.

Step 2: Specify the population size (*NP*), maximum generation limit (*maxgen*) and crossover and mutation probabilities.

Step 3: The *N*P chromosome population are randomly initialized.

Step 4: Evaluate the fitness (*fit*) of each initial chromosome using Eq. (7) and find the current best fitness (*bestfit*) and current best chromosome (*Bchrom*) and set the best old fitness (*Bold*) $=$ *bestfit* .

Step 5: Set generation counter (*gen*) = 0 and same result counter (*S*) = 0.

Step 6: If $gen < maxgen$ and $S < 200$, set chromosome counter (*k*) = 1. Otherwise, go to Step 7.

Step 6.1: Set the initial current chromosome ($chrom_1^{gen+1}$) by randomly selecting it from the previous generation.

Step 6.2: If $k < NP$, calculate $\Delta fit = fit(chrom_k^{gen}) - fit(chrom_{k+1}^{gen})$, set $T_0 = NP$. Otherwise, go to Step 6.3.

Step 6.2.1: If $\Delta fit \geq 0$, set $chrom_{k+1}^{gen+1} = chrom_k^{gen}$ and go to Step 6.2.3.

Step 6.2.2: If $\exp(\Delta fit / T_P) > \text{random}(0,1)$, set $chrom_{k+1}^{gen+1} = chrom_k^{gen}$, where $T_P = T_0 / k$. Otherwise, set $chrom_{k+1}^{gen+1} = chrom_1^{gen+1}$.

Step 6.2.3: $k = k + 1$, return to Step 6.2.

Step 6.3: Set the chromosome replacement counter $(k_1 = 1)$.

Step 6.4: If $k_1 \leq \lceil 0.2NP \rceil$, randomly generate $rp \in \{1, ..., NP\}$. Otherwise, go to Step 6.5.

Step 6.4.1: Set $chrom_{rp}^{gen+1} = Bchrom$.

Step 6.4.2: $k_1 = k_1 + 1$, return to Step 6.4.

Step 6.5: Perform the crossover.

Step 6.6: Perform the mutation.

Step 6.7: Evaluate the *fit* of each offspring and find the *bestfit* and *Bchrom* .

Step 6.8: If $bestfit = Bold$, $S = S + 1$. Otherwise, $S = 0$.

Step 6.9: Set $Bold = bestfit$.

Step 6.10: Set $gen = gen + 1$, return to Step 6.

Step 7: The *Bchrom* is the final solution.

4. NUMERICAL AND PLACEMENT RESULTS

The results of optimal placement of PMU and RTU for multi-areas power system state estimation can be handled the bad data detection in any single measurement, since the measurement system is critical measurement free. These numerical results are show as follows.

Table 1. Numerical results of optimal placements of PMU and RTUs

System	Area	PMU bus Location	No of RTUs		No. of conventional Measurement Pair		Cost	
			HGS	SA	HGS	SA	HGS	SA
10-bus	0	2	3	3	7	7	331.5	331.5
IEEE 14-bus	1	4	1	1	3	3	113.5	113.5
	2	6	3	3	7	7	331.5	331.5
IEEE 118-bus	1	12	5	5	10	10	545	545
	2	17	8	8	20	20	890	890
	3	37	5	5	16	16	572	572
	4	32	6	7	20	17	690	776.5
	5	75	5	5	15	15	567.5	567.5
	6	49	7	7	20	20	790	790
	7	100	4	4	10	10	445	445
	8	80	5	5	18	18	581	581
	9	59	6	6	17	17	676.5	676.5

In Table 1, each area with tie line is observable with critical measurement free. Since HGS yields the lower cost than SA that shows in the area 4 of IEEE 118-bus, the computing time does not required to concern. Typical placements are shown as follows.

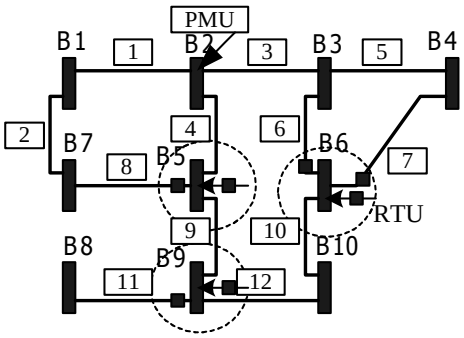

Fig. 1. Typical PMU and RTUs placement for 10-bus system with 1 area

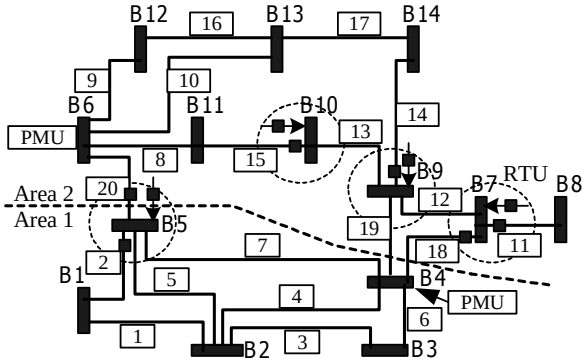

Fig. 2. Typical PMUs and RTUs placement for IEEE 14-bus system with 2 areas.

5. CONCLUSION

Optimal placement of PMU and RTUs is required for multiareas power system state estimation. PMU is placed at the first bus with the maximum number of line incidents. HGS is used to optimize the conventional measurement and RTU placement for area observable with critical measurement free. At the PMU buses, the injection current measurement should be placed to handle the flow current measurement loss of PMU. The measurement placement results are reasonable, since the total number of power flow measurement pair and current measurement are equal to at least as the number of area system buses.

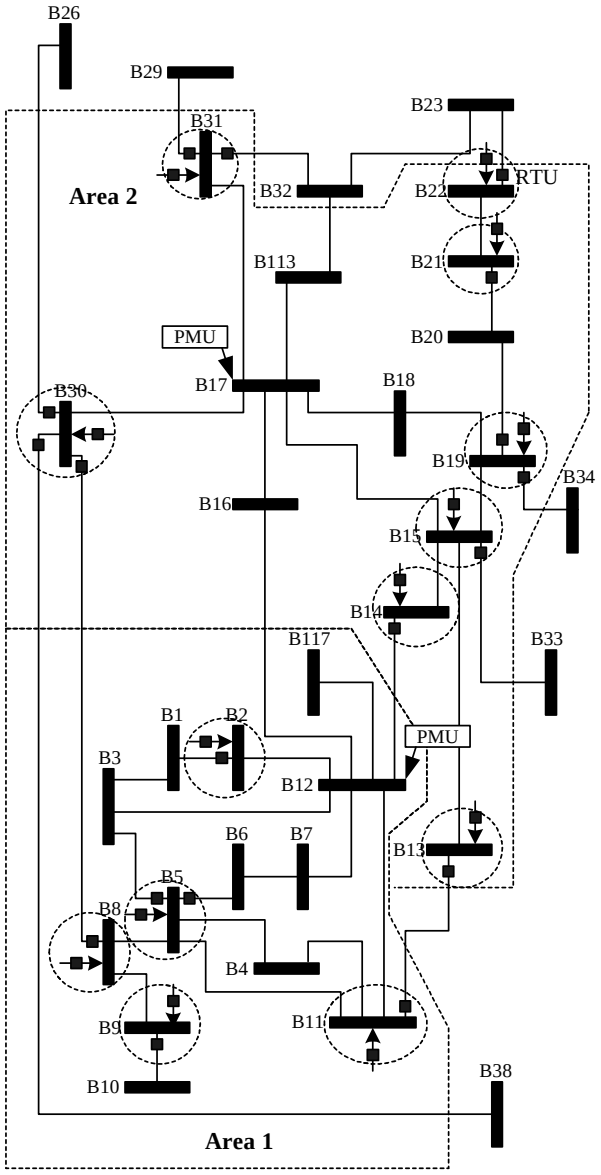

Fig. 3. Typical PMUs and RTUs placement for areas 1 and 2 of IEEE 118-bus system.

REFERENCES

[1] Zhao, L. and Abur, A. 2005. Multiarea State Estimation Using Synchronized Phasor Measurements. *IEEE Trans. Power Syst.*, vol. 20, pp.611-617.

[2] Cutsem, T. V. and Ribbens-Pavella, M. 1983. Critical Survey of Hierarchical Method for State Estimation of Electric Power System. *IEEE Trans. Power App. Syst.*, vol. PAS-102, pp.3415-3424.

[3] Yoon, Y. J. 2005. Study of the Utilization and Benefits of Phasor Measurement Units for Large Scale Power System State Estimation. M. Sc. Thesis of Texas A&M University.

[4] Rakpenthai, C. Premrudeepreechacharn, S., Uatrongjit, S. and Watson, N. R. 2005. Measurement placement for power system state estimation using decomposition technique. *Electric Power Systems Research*, vol. 75, pp. 41-49.

[5] Mili, L., Baldwin, T. and Adapa, R. 1990. Phasor Measurement Placement for voltage stability analysis of power system. In *Proc. The 29th conference on Decision and Control*, pp.3033-3038.

[6] Khatip, A. K., Nuqui, R. F., Ingram, M. R. and Phadke, A. G. 2004. Real-time Estimation of Security from Voltage Collapse Using Synchronized Phasor Measurements. In *Proc. IEEE PES General Meeting*, pp.582-588.

[7] Kerdchuen, T. and Ongsakul, W. 2007. Optimal Measurement placement for Security Constrained

State Estimation Using Hybrid Genetic Algorithm and Simulated Annealing. Online in *European Trans. on Electrical Power*.

[8] Kerdchuen, T. and Ongsakul, W. 2008. Optimal PMU Placement by Stochastic Simulated Annealing for Power System State Estimation. *GMSARN International Journal*, vol. 2, no. 2, pp. 61-66.

[9] Filho, M. B. D. C., de Souza, J. C. S. and Oliveira, F. M. F. 2001. Identifying Critical Measurements & Sets for Power System State Estimation. Present at *IEEE Porto Power Conference*, Porto, Portugal.

[10] Chen, J. and Abur, A. 2006. Placement of PMUs to Enable Bad Data Detection in State Estimation. *IEEE Trans. Power Syst.*, vol. 21, no. 4, pp.1608-1615.

[11] Filho, M. B. D. C., de Souza, J. C. S. and Oliveira, F. M. F. 2001. Identifying Critical Measurements & Sets for Power System State Estimation. Presented at *IEEE Porto Power Conference*, Porto, Portugal.

Review of Existing Energy Framework for Vietnam

Tien Minh Do, Deepak Sharma and Ngoc Hung Nguyen

***Abstract*—** *Since introducing a market-orientation to the economy in 1986, Vietnam has made considerable socio-economic progress. For example, over the period 1986-2007, the GDP of Vietnam has grown at approximately 7 per cent per year which is the highest growth rate in the ASEAN region. In this growth, the country's energy sector has played a vital role. This role is likely to deepen in the years to come as Vietnam strives to achieve ever higher economic progress. Such deepening in the role of energy, this paper argues, will heighten concerns about the security of energy supply, increased CO2 emissions and pollution and other social and political challenges. In order to address these challenges, Vietnam has over the last decade, initiated several energy policies underpinned by appropriate legislation – called, 'institutional framework', in the context of this paper. A deeper review of this framework suggests that it is typified by a lack of cohesiveness of policy direction and purpose, fragmented institutional structures and responsibilities, and weak public constituency on environmental issues. The existing framework is therefore unlikely to be able to provide a satisfactory redress to the challenges noted above. This paper provides some suggestions to reduce the weaknesses of the existing framework. These include: articulating the significance of the link between energy, economy and environment; developing coherence in institutional purpose and design, and raising public awareness through better communication and education.*

***Keywords*— Energy policy, energy demand and policy framework.**

1. INTRODUCTION

Vietnam - a developing country - began a transition from a centrally planned to a market economy in 1986. This process accelerated in 1989, with the devaluation of the Vietnamese currency (VND) and the decontrol of most prices. In 1993, Vietnam obtained access to concessional international finance and the US embargo was lifted in 1994. Vietnam became a member of the ASEAN, APEC and WTO in the years 1995, 1998 and 2007, respectively. All these developments provided stimulus to the economy, which has responded with a growth of more than 7% pa over the past fifteen years – the highest growth rate in the ASEAN region [1]. It is expected that these growth trends will continue in the years to come. In this growth, the country's energy sector, which also provides approximately one fourth of the nation's foreign earnings [2], will play a vital role. This role will however be negotiated in the backdrop of several challenges including: (i) ensuring security of energy supply for socio-economic development, (ii) protecting the natural environment from possible damage caused by energy activities, and (iii) addressing social and political issues, for example, equity, justice and transparency.

In order to address these challenges, Vietnam has, over the last decade, initiated several policies, underpinned by appropriate legislation, for example, Petroleum Law (1993, amended 2000), Environmental Protection Law (2005), Mineral Law (1996, supplemented and amended 2005), Electricity Law (2005), and National Policy on Energy Conservation and Efficiency (2006). In addition, several institutions, for example, Electricity Regulatory Authority of Vietnam (ERAV) and National Environment Agency (NEA) have been established to implement these policies.

These energy and environmental legislation and institutions constitute – in the context of this paper – the institutional framework for energy sector. This framework provides the ambit within which the country's energy sector will evolve. This paper argues that this framework – notwithstanding the policy development of the last few years is still not adequate for addressing the challenges faced by the energy sector, as noted above. There is therefore a need to examine the efficiency of this framework so that its weaknesses could be overcome. This paper attempts to do that. The paper starts with a description of the challenges faced by the Vietnamese energy sector. It is followed by an examination of limitations of the existing energy and environmental framework. Finally, some suggestions are made for improving the framework.

2. CHALLENGES FACED BY VIETNAMESE ENERGY SECTOR

In fuelling Vietnam's development, the country's energy sector is likely to face the twin challenges of ensuring security of energy supply while protecting the environment. The key factors that are likely to contribute to worsening the security of energy supply include: (i) foreseeable energy import dependency in a situation of increasing energy demand and limited indigenous

Tien Minh Do (corresponding author) and Deepak Sharma are with Energy Planning and Policy Program, Faculty of Engineering, University of Technology, Sydney (UTS), Australia. Tel: +61 2 9514 2631; Email: tmdo@eng.uts.edu.au.

Ngoc Hung Nguyen is with Dept. of Energy Economics, Demand Forecast & DSM, Institute of Energy Vietnam, N^0 6 Ton That Tung Street, Hanoi, Vietnam. Tel: +844 8523351.

supply; (ii) continuing low energy efficiency, due mainly to poor infrastructure, provision and operation and management practices; and (iii) a shortage of funds for developing energy infrastructure. And the environmental concerns are likely due to the significant contributions that rapidly evolving energy sector is expected to make in term of increased pollution, CO2 emissions and deforestation. Further discussion of these issues is presented in the remainder of this section.

2.1 Security of energy supply

Foreseeable energy import dependency

There is a general consensus among the Vietnamese policy makers and planners that the indigenous energy resources of Vietnam are unlikely to be able to meet the increasing energy demand of the nation. For example, over the period 1990 and 2006, the commercial final energy demand increased from 4217 to 28049 KTOE – an annual growth rate of 12.5% [3]. The corresponding annual growth rates of GDP and population over this period were 7.5% and 1.6%, respectively [1]. In order to sustain an GDP annual growth of 8.4% over the period 2005-2025, it is estimated that the final and primary energy supply must grow by 8.8% and 9.5% per annum, reaching 123,000 KTOE and 170,000 KTOE, respectively in the year 2025 – about six times as compared to their 2006 levels (see figure 1).

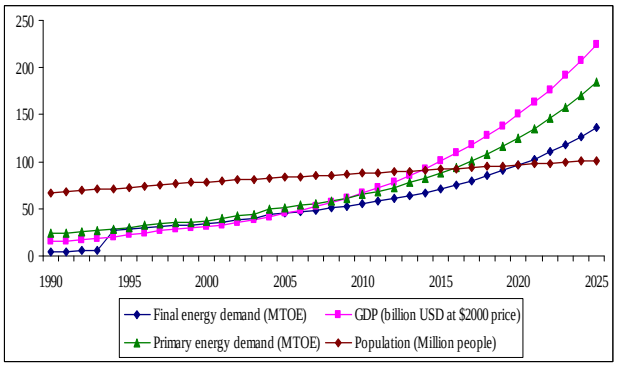

Source: IEA, (2007) [1], IEA, (2007) [3] and JICA, (2008) [4]

Fig.1. Energy demand, GDP and population

The industry, transport and residential sectors collectively accounted for 90% of total final energy consumption in the year 2006. Among three biggest energy consumers, the energy consumption shares of these sectors are 42.8, 30.9 and 16.2%, respectively [3]. The inter-sectoral trends in energy consumption are expected to undergo significant changes in the coming years. For example, the industry sector is expected to have the highest growth rate in final energy consumption. It is estimated to account for nearly 57.6% of total final energy consumption by 2025. This is due to the government's policy emphasis on industrialisation to promote economic development. At the same time, the shares of the transport and residential sector are expected to account for 19.8 and 16.2%, respectively. Most of the increased energy demand in transport will be attributable to the road sub-sector as a result of increase in per capita driving activity and vehicle population. The residential sector is characterized by increase in commercial energy demand due to improvement of access to modern energy and people's income [4] (see figure 2).

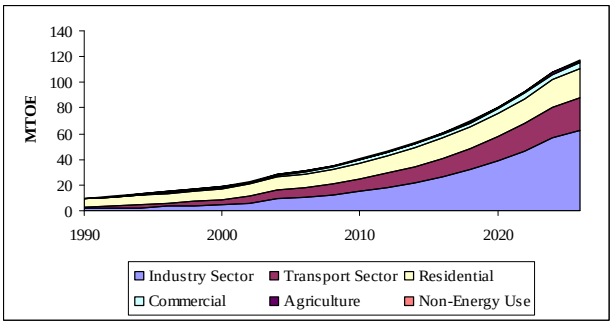

Source: IEA, (2007) [3] and JICA, (2008) [4]

Fig.2. Final energy demand by sector

In terms of fuel types, coal and oil accounted for the largest shares of commercial primary energy resources, collectively accounting for 75% of the total, followed by hydro and gas with a share of 25%. The shares of coal, gas and petroleum have tended to increase while the share of hydro has decreased over the period 1990 and 2025. In the year 2006, the shares of coal, oil, gas and hydro in total primary energy supply were 31.5, 43.5, 17.8 and 7.2%, respectively. Between 1990 and 2006, gas grew at the fastest annual rate (of 70%) driven largely by the start-up of natural gas supply from Nam Con Son Basin to Phy My electricity complex in 2002. During the same period, oil products grew at the second fastest rate of 10.5% due to the growth in transportation and industry. Hydro and coal grew at 10 and 9% respectively as a result of high demand for electricity generation [3].

Table 1: Primary energy demand

MTOE

	2005	2010	2015	2020	2025
Coal	8.79	12.98	23.92	36.27	73.19
Oil	12.01	17.29	26.80	40.70	59.47
Gas	5.60	8.94	11.65	20.67	26.51
Hydro	1.40	2.98	4.50	5.41	5.48
Nuclear	0	0	0	0.88	2.11
Renewable	0.06	0.19	0.40	0.57	0.70
E. import	0.01	0.41	0.69	2.13	2.14
Bio-mass	14.69	14.18	13.48	12.43	10.60
Total	27.86	42.33	67.95	106.65	169.60

Source: JICA, 2008) [4]

In the future, Table 1 shows that fossil fuels will continue to dominate the future primary energy mix, accounting for approximately 90% of total commercial primary energy demand. Excluding large-scale hydro,

other types of new and renewable energy sources, such as mini-hydro, wind and solar, will continue to be promoted, raising their share to 3.5% by 2025. Nuclear power – expected to be introduced by the year 2020 – is estimated to account for 1% of total energy demand by 2025. The share of biomass in total primary requirements is expected to decrease sharply, from 46.3% in 2006, to 6% in 2025 [4] (see figure 3).

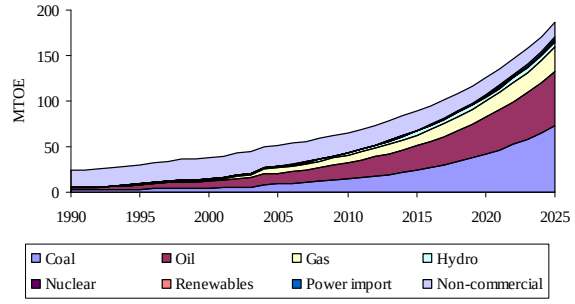

Source: IEA, (2007) [3] and JICA, (2008) [4]

Fig.3. Primary energy demand by fuel type

On the supply side, Vietnam is endowed with several energy resources including coal, oil, natural gas, hydro and renewable and it has generally been an energy-self-sufficient economy. The growth rate of domestic energy production for the period 1990-2006 was 14.5%, making the energy-economy elasticity equal to 2.0. Over this period, indigenous oil and gas production grew at the highest rate (16% per year), followed by coal (14.3% per year). In 2006, total domestic energy production was 47699 KTOE of which the shares of coal, oil, gas and hydro were 44.5%, 38%, 13.2% and 4.3%, respectively. At the same time, the total domestic primary energy supply (net of domestic imports and exports) in 2006 was 28049 KTOE [3]. However, as the future energy demand escalates in order to sustain the country's socio-economic development, there are concerns about energy security. These concerns get further heightened if one takes note of the fact that Vietnam currently does not have any meaningful stockpiling policies. This could clearly raise energy supply reliability issues in the future.

Table 2. Energy reserve and potential exploitation

Energy source	Proven reserve	Potential of exploitation per annum
Coal	6.00 (Bill. tons)	60 – 80 (Mill. tons)
Oil	615 – 957 (Mill. tons)	25 – 30 (Mill. tons)
Gas	600 (Bill. cubic m3)	15 – 30 (Bill. cubic m3)
Hydro	20 (GW)	80 (Bill. Kwh)

Source: Ministry of Industry, (2006) [5], JICA, 2008) [4] and Institute of Energy (IE), Vietnam (2008) [6].

Table 1 shows the precariousness of the future resource situation in Vietnam. For example, with the estimated exploitable capacity of 25 millions tons of crude oil and 15 billions cubic meters of natural gas per annum, reserve of oil and gas will not be enough for extraction in 30 years. Further, despite abundance of hydro potential, this energy resource will solely depend on the amount of rain-fall that is increasingly being affected by global warming. In addition, some new and renewable energy sources such as wind and solar are unlikely to reach commercial exploitability in the foreseeable future. In the area of electricity production, the situation is quite serious. Due to a thin system reserve and seasonal dependency, the electricity system has been experiencing power shortages recently. Power cuts, especially in the dry season have become commonplace. In the case of petroleum products, Vietnam – despite being a net exporter – still has to import its entire requirements of refined petroleum products to meet the domestic demand because the first refinery with a capacity of 6.5 million tons per year is planned to be put in operation in 2009; and the second refinery with total annual capacity of 10 million tons is scheduled for commissioning in 2015. Besides, the lack of stockpiling also makes the Vietnam's energy supply system highly vulnerable to change in the world's energy market, especially when there is an oil supply disruption due to geopolitical conflicts [7].

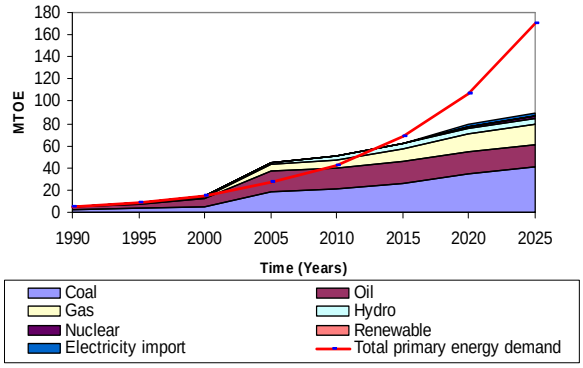

Source: IEA, (2007) [3] and JICA, (2008) [4]

Fig 4. Primary energy supply and demand balance

As can be seen in figure 4, with rapidly increasing energy demand and limited indigenous supply Vietnam is expected to become a net energy importer within the next decade. It is projected to import 48.6% of its total commercial primary energy needs by the years 2025. Among fuels import at the same time, coal, oil and gas are expected to account for 18.8%, 23.4% and 5.1%, respectively. Besides, electricity import also contributes to 1.3% of total commercial primary energy requirement [4]. This will lead to a substantial change in the Vietnam's energy structure. Appropriate energy policies are therefore needed to achieve a balance in the sources of energy supply and to avoid energy supply disruption caused by geopolitical disputes. For example, along with diversity of energy import sources, new and renewable energy, such as nuclear, solar and wind would play role

in ensuring security of energy supply for Vietnam in the future.

Low energy efficiency

Low energy efficiency (at demand and supply sides) is a major energy challenge facing Vietnam. The major sources of such inefficiency include: old technologies and poor energy management practices, from conversion to processing and end-use levels. Indeed, only new, large-scale combined-cycle natural gas-based power plants incorporate world-class technology and provide high fuel efficiency. Most existing coal and oil-fired plants have low fuel efficiency as their facilities and technology are relatively old. In 2005, energy loss in power generation amounted to 9.5 % of total primary energy consumption [3]. In 2008, transmission and distribution loss accounted for 9.35% of total electricity output [8]. The same explanation could be applied for the demand side. Old technologies such as imported second-hand vehicles and domestically-made electrical appliances are responsible for high fuel and electricity consumption. Indeed, both primary and final energy intensities of Vietnam are conspicuously higher as compared with almost all ASEAN and OECD countries. For example, in 2005, the country's primary energy intensity was 0.23 KgOE/USD while ASEAN and OECD averages were 0.2 and 0.18 KgOE/USD, respectively. Similarly, on the demand side, the final energy intensities were 0.2 KgOE/USD, 0.16 KgOE and 0.12KgOE for Vietnam, ASEAN and OECD countries, respectively [1].

Funding constraints

A very large sum of money is needed for developing Vietnam's energy infrastructure including system expansion and efficiency improvement. Total investment requirements for this purpose over the period 2000-2025 are projected to be of the order of USD 136-172 billion. The majority of these investments will be required for the electricity sector alone. Oil and gas investments will be next, accounting for 15% of total capital investment requirements (see figure 4).

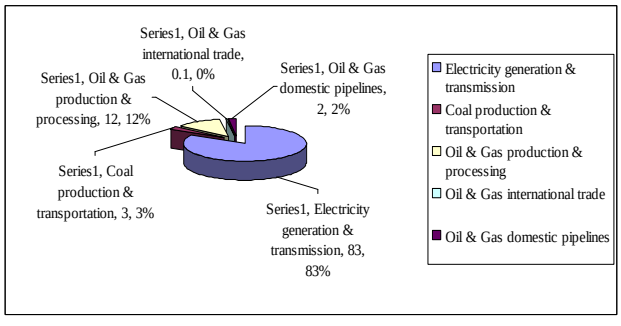

Source: APECRC, (2006) [9]

Fig.5. Investment requirements for energy sector infrastructure development.

As a percentage of GDP, Vietnam's cumulative investment requirements for the energy sector will be between 4.2 and 5.3 per cent over the period 2000-2025, the highest level in the ASEAN region. For the ASEAN economies, the average investment requirements as a percentage of GDP range between 1.2 and 1.5 per cent [9]. Clearly, the mobilization of sufficient funds for developing the energy sector is expected to remain a major challenge for a poor, developing country like Vietnam where money is always hungry for many other critical programs, such as poverty reduction, education and primary health care services in the remote areas. The situation is even getting worse if one takes note of the negative impacts of the current world economic crisis. At present, Vietnam is a net energy exporter. The revenues are likely to reduce because of lower energy prices resulting from decreasing world energy demand. This is likely to cause difficulties not only for the state budget as revenue from energy exports form a large share of the nation's foreign earnings but also for the energy sector development because of the weakening financial status of the energy businesses. Further, the world economic crisis is expected to reduce the flow of foreign investment to Vietnam's economy in general. Finally, low efficiency of investment in the energy sector, especially the power industry due to unreasonable cross-subsidized electricity tariffs, is also responsible for poor mobilization of capital flow of this sector. It is interestingly indicated by the fact that while the Electricity of Vietnam (EVN) – the state entity who is in charged of developing power system – does not have enough funds for the system capacity expansion but still invests in highly profitable sectors, such as stock market and telecommunication. [8]

2.2 Environment

Vietnam is currently one of the lowest per capita emitters of carbon emissions. In 2005, the country's CO2 emissions per capita were 0.97 tons - 23% of the world average. At the same time, however, CO2 emissions per unit of GDP are very high - about 2 times the world average [10]. This suggests that energy is not being effectively used for economic activities in Vietnam. Consequently, the natural environment suffers. Further, the CO2 emissions are expected to grow rapidly as Vietnam industrialises and the economy utilises more carbon intensive fuels, substituting traditional non-commercial fuels including biomass. On average, the CO2 emissions are projected to increase at an annual rate of 8.5% and could reach 400 million tons by 2025 (see figure 5) [4]. Major sources for such emissions are energy, industry and transport sectors, accounting for more than 85% of total CO2 emissions. In addition, energy extraction and transportation, such as coal mining in the North and oil exploitation in the South, that have not been well planned and are likely to contribute to adverse environmental outcomes. For example, the high density of the open-pit coal mining activities in Quang Ninh province has caused considerable soil erosion in this region. As a result, the Ha long Bay nearby – a World's natural heritage site – is affected by dust and waste water pollution.

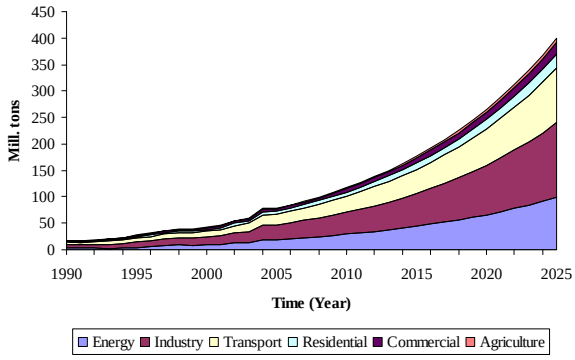

Source: IEA, (2007) [11] and JICA, (2008) [4]

Fig.6. CO2 emissions by sector.

3. EXISTING ENERGY POLICY SETTINGS IN VIETNAM

This section reviews the existing energy policy settings of Vietnam, especially the extent to which such policies are likely to be able to address the energy challenges discussed in the previous section of the paper.

3.1 Energy security policies

With a poor energy infrastructure and limited energy resources, Vietnam is expected to move from being a net energy exporter to a net energy importer within the next decade. In order to redress this issue, the Vietnamese government has taken a suite of policy measures including:

a) strengthening domestic energy supply capacity, through legislative reforms, and expanding the energy infrastructure to reduce dependence on imported energy that is prone to volatility, especially petroleum.

b) applying preferential policies for financing and widening international cooperation in order to strengthen exploration and development of indigenous resources thereby firming-up reserves and increasing exploitability of oil, gas, coal and new and renewable energy;

c) supporting Vietnam's national oil company to invest in the exploration and development of oil and gas resources overseas;

d) intensifying regional and international energy cooperation and diversifying energy import sources; and

e) developing clean fuels, especially nuclear and renewable energy [5].

These policies are supported by an institutional framework that includes elaborate laws and institutions. For example, The Common Investment Law and The United Enterprises Law, that became effective from 1 July 2006, encourages foreign and domestic organisations and individuals to invest in power production through Build-Operate-Transfer (BOT) arrangements; and projects in remote areas have been accorded preferential treatment under this law and tax exemptions are given for imported machine and equipment. With promulgation of the Mineral Law in 1996, the Amended Petroleum Law in 2000, and the Electricity Law in 2005, the legislative environment for businesses in the energy sector has been set up and a legal framework for formulating policies and regulations, such as policy on upstream oil and gas to enhance energy security, has been created. The Vietnamese government also promotes development of new and renewable energy in order to diversify energy sources, improve access to modern energy in off-grid areas, and to reduce negative environmental impacts of energy activities through Renewable Energy Action Plan. In addition, Vietnam is a participant in international and regional cooperation ventures, such as the Great Mekong Sub-region and oil and gas exploration in Mongolia, Indonesia, Malaysia, Iraq, Algeria, Russia, Peru, Venezuela and Cuba to stabilise energy import [11].

Notwithstanding these initiatives, the objective of ensuring energy supply security set by the government is unlikely to be easily achieved – this paper contends. This is due to the weaknesses of the existing policies on energy market, energy pricing and energy efficiency. At present, the national government is responsible for ensuring the security of energy supply and regulating most energy prices. The lack of a united domestic energy market and rational energy pricing mechanism has prevented players, including private investors entering the energy market. Hence, the role of private sector in energy security of Vietnam is limited. Consider the case of power generation as an example. In this sector, prices for power supply rise and fall in accordance with interplay of market forces, but the end-user prices are fixed by the government. The utilities in the middle are, therefore, in position to be either squeezed into bankruptcy or gain undue profits. In the long-term, therefore, the security of energy supply should not be seen as a national responsibility but a common one shared among government, energy firms and wherever applicable, individual consumers through a market mechanism. The security of energy supply could be ensured through a united domestic energy market where the government establishes the objectives and set the rules that enable firms, both state-owned and private ones to achieve those objectives. One may argue that a market-based energy system could reduce the security of energy supply and impose new risks, such as those associated with reserve capacity or consistency with environmental or economic objectives. In fact, the market could enhance the security of energy supply by increasing the number of market participants and improving the flexibility of energy system because market makes the costs of security of energy supply more transparent, which in turn can lead to a situation where consumers are prepared to pay a premium for increased security of supply or to accept a reduced level of security in exchange for lower prices. Moreover, the main effect of the market-based energy system is that it can shift the prime responsibility for achieving the security of supply from government towards market participants. This could reduce the financial pressures on

the government, for mobilising investment capital for energy infrastructure development. In addition, a competitive market could lead to an effective allocation of resources, both demand and supply sides and hence improvement of energy efficiency [12].

3.2 Energy market reform policies

In fact, the energy market in Vietnam has been developed since the country started the market-oriented economy in 1986. The purpose of developing a united energy market, both domestically and internationally is to promote investment and secure financial resources for sustainable development of the energy system. The energy market development in Vietnam is a process to move from the system of direct market control via the state firms to the system in which the energy supply and demand is decided by the market under the rules to ensure fair and efficient competition. In this process, Vietnam has achieved some important results. For examples: (i) In the down-stream markets for coal, oil and gas the prices of these fuels are set at the international prices; (ii) Private investors are encouraged to participate in energy activities, such as power generation and petroleum products trade; And (iii) Along with the Electricity Law, Vietnam has set up a roadmap that includes three phases for power market development [13]. According to this roadmap, the first phase for a competitive power generation market is scheduled to start in 2009 and complete in 2014. It is followed by the second phase that is competitive market in bulk power, from 2014 to 2022. Finally, the third phase that is a competitive retail power market will take place from the year 2022. However, there are still some obstacles to realization of the efficient energy market in Vietnam. First, the prices of coal and natural gas that are locally produced are substantially lower than international prices while prices of the imported petroleum products are at the international levels. Further, the electricity tariffs are still regulated by the Central government with so much cross subsidies. Such distorted energy price system would, in turn cause distortion to the energy market system and energy structure. In addition, unfair competition resulted from dominance of the state enterprises with advantage of controlling the existing energy businesses and having market penetrated information. Therefore, along with the deregulation process of energy market, some measures, such as, monopoly prevention, equitization and privatization are needed for developing an efficient energy market [4]

3.3 Energy efficiency policies

Among the ASEAN fraternity, Vietnam is one of the lowest per capita energy consuming countries, and it is one of the highest energy-intensity countries. This suggests that energy efficiency in Vietnam at the final user and conversion sectors is low. Such inefficiency continues to cause considerable, adverse economic and environmental impacts. This recognition has prompted the Vietnamese policy makers to develop a national program aimed at enhancing an effective use of energy, with emphasis on both, the supply and demand sides. This program envisages a saving of 3 to 5 per cent, and 5 to 8 per cent, of the total energy consumed nationwide, for the periods 2006-2010 and 2011-2015, respectively. Some key initiatives to achieve this include:

a) developing a legal framework for economical and efficient use of energy in industrial production, in management of construction projects, and in energy-using equipment;
b) raising people's awareness about the economical and efficient use of energy through public propagation and education programs;
c) conducting a pilot campaign on "Building a model of economical use of energy in every household"
d) developing standards and using energy-saving product labels on selected appliances;
e) providing technical assistance for local manufacturers that comply with energy consumption standards;
f) building management models on economical and efficient use of energy for enterprises;
g) assisting enterprises in upgrading, improving and optimising their production chains for the economical and efficient use of energy; and
h) capacity building and deployment of activities that enhance the economical and efficient use of energy in construction, designing and management of buildings [5].

Despite these initiatives of the Vietnamese government, the results in terms of energy efficiency improvement are rather modest. This, this paper argues, is due to the following inadequacies of the existing policy settings. Firstly, the policy emphasises the promotion of effective management measures and advanced technologies, in both supply and demand sides, but sufficient time is not given for the uptake of these technologies. For example, typical useful life time of the energy technologies, particularly the electricity generation plants, is 30-40 years, but the Vietnamese program on energy efficiency aims to achieve savings of 5 to 8% within 5 years (from 2011 to 2015). To meet this target, almost all old coal-fired plants must be retired. It is clearly impracticable, especially where huge investment is needed every year in the power sector in order to meet the increasing electricity demand. The current government program is clearly too ambitious. In fact it was formulated without due consideration of the country's economic conditions and the long-term perspective required when analysing the energy infrastructure and policy issues. Secondly, it is widely known that there is a link between policies on energy efficiency and other policies such as energy pricing and environmental protection. At present subsidies are uniformly distributed among various income groups, instead of focusing on improving the affordability of energy for the disadvantaged groups. There is, therefore, no incentive for the rich to save energy. Besides, the cross-subsidies contribute to making the industry less competitive, due to the relatively high unsubsidised

energy prices they have to pay. Next, the lack of focus on managing the energy consumption growth, for example, cooling and airconditioning could constraint the effectiveness of the program.

3.4 Energy pricing policies

Because energy has until now been seen as a strategic good, the pricing of most fuels has been regulated directly through the Prime Minister's Office. The State Pricing Committee (SPC – recently renamed Price Control Department under the Ministry of Finance) first evaluates the energy prices proposed by various energy enterprises and then submits them to the Prime Minister's Office for approval. Prices of most energy fuels are cross-subsidised. This sends a wrong signal to the users; and the lower the energy prices results in higher energy consumption, leading to reduced security of energy supply, decreased energy efficiency and damage to the environment. In addition, industries that pay for subsidies become less competitive in the market due to increase in their production costs resulting from high-priced energy inputs. Furthermore, the prices regulated by the government do not reflect production costs and the supply-demand relationship in the energy market, especially the long run marginal costs (LRMC), get distorted. As a result, the utilities are placed in a difficult financial position and it, in turn, prevents the mobilisation of adequate investment capital for the energy sector. Thus, there is an imminent need for Vietnam to develop a rational energy pricing mechanism that would encourage energy security and energy efficiency, through a transition from centrally administered philosophy to a system of transparently regulated rules for the market players [7].

3.5 Environmental policies

In 1991, Vietnam approved a detailed environmental plan called the National Plan for Environment and Sustainable Development (Ministry of Science and Technology 2006). The plan provides a comprehensive framework for establishing the strategies, policies, institutions, laws, regulations and programs needed to address environmental issues. The governing law on environmental protection came into force in 1993. This policy and legislation aim to develop the energy sector while promoting a clean environment. Specific objectives of the program are to:

a) determine long term objectives for energy and the environment in line with regional environmental standards;
b) establish financial rules on energy and the environment to ensure that the costs of all factors relating to the protection of the environment are taken into account;
c) implement efficient technologies to reduce pollution in energy exploration, transportation, processing and use; and
d) implement safety measures and avoid pollution of air and water during the operation of gas pipelines and transportation and use of crude oil [14].

These initiatives, laudable though they are, have so for hat limited impact on controlling environmental degradation. It also appears that this policy framework is unlikely to be able to withstand the environmental consequences of rapidly increasing energy consumption for achieving economic prosperity in the future. Some of the major reasons behind the inability of the existing environmental policies are discussed as follows. Firstly, the existing environmental policies appear to have been formulated in isolation, without carefully analyzing their wider impacts on the economy and society. In other words, they do not reflect the close relationship that exists between economy and the environment, thus limiting their ability to appropriately articulate and redress the issues that emerge at the interface of these three segments of the economy. The following discussion provides support for this argument:

e) While the National Environmental Action Plan (NEAP) emphasises the importance of CO2-mitigating options such as energy efficiency and penetration of low carbon technologies (renewable, nuclear and natural gas), there is however no consideration in the plan of other economic instruments, for example carbon taxes or tradable permits to reduce demand for energy. These policy instruments are currently viewed world-over to be quite effective in containing the growth of CO2 emissions, on the grounds that they provide incentives to the firms to operate at economic optimum levels while ensuring superior environmental outcomes. The experience with the cap-and trade scheme for trading carbon emissions in Europe and sulphur-dioxide in America is often cited to support this argument. One might argue that such market-based instrument are not appropriate for Vietnam at this stage of development, as is perhaps tacitly recognised by the non-inclusion of developing countries in the list of those required to limit CO2 emissions in Kyoto Protocol [15]. The high cost associated with the setting up of a system to implement these instruments is obviously a factor behind such viewpoint. However, the environmental impacts of energy activities are rapidly becoming obvious and Vietnamese policy makers will need to examine these instruments – as implicit in the Bali Agreement [16].
f) The Environmental Law of Vietnam is founded on the Polluter Pays Principle (PPP) as defined and adopted by the Organisation of Economic Cooperation and Development (OECD) in 1972. This principle requires that polluters to take action to protect the environment and to support all related costs. It also places the environmental authorities in the positions of enforcer and controller, not as executor. For the energy sector, if the carbon tax is applied in the future, this principle would stimulate a change in the structure of generation and drive the costs of electricity upwards. The economy would consequently face

difficulty to make rapid adjustments, especially in an inflationary economic environment. In contrast, the Shared Responsibility Principle (SRP), based on direct and indirect energy consumption, has some advantages compared to the PPP. Over the long-term, adopting this principle would lead to a more sustainable energy system, by gradually moving away from fossil fuel-based technology to cleaner technology. It would also even-handedly distribute the economic burden and encourage both energy producers and consumers to improve energy efficiency. However, in the short and medium terms, this principle has a relatively smaller impact on carbon-dioxide reduction. A careful analysis of these options is however needed before the country decides on its environmental strategies.

g) Most environmental standards in Vietnam are set based on ISO 14000, without consideration of their wide impacts. For example, recently the Environmental Protection Department has proposed to apply the EURO-2 standards for vehicle exhaust emissions [17]. However, if this proposal was approved, about 50% of total number of vehicles in Vietnam would have been prohibited from operations. This would obviously have caused the collapse of the transportation system and hence serious set back for the economy. The economic and environmental benefits of such strict standards fall far short of the costs and that would make these standards seldom enforceable.

h) Recently, the Vietnamese Government has used energy pricing policy, especially electricity prices, to regulate electricity demand by applying accumulated prices for different levels of electricity consumed, and to improve access to modern energy of the poor through cross-subsidies. This would lead to a distortion of supply-demand relation and cause other economic and environmental consequences. For example, due to cheap energy prices, some high energy intensive sectors like the steel and iron industry would not invest in improving their technologies to reduce energy consumption. As a result, energy demand would increase, leading to adverse environmental outcomes.

Secondly, poor management practices in Vietnam also limit the effectiveness of the country's environmental policies. Some factors contributing to such limitation include:

i) Wide dispersion of environmental responsibilities and poor inter-sectoral and inter-agency cooperation and coordination. Currently, two ministries in Vietnam are responsible for environmental management, namely, the Ministry of Natural Resources and Environment (MONRE) and the Ministry of Planning and Investment (MPI). Within the MONRE, the National Environmental Agency takes the lead on environmental management and implementation issues. In the MPI, the Department of Science, Technology and Environment oversees environmental issues within the context of national development plans and budgeting exercises. The provincial offices of the department are responsible for planning. The links between MONRE and MPI, and with other ministries involved in formulating and implementing environmental polices, is weak, and somewhat undefined. For example, the Ministry of Industry and Trade (MOIT) has first-line policy and supervisory responsibilities for the energy sector but it does not participate in making any laws, regulations or standards related to environmental protection in the energy sector. In addition, there are some jurisdictional overlaps between various environmental agencies. This often results in conflicts, for example, the National Environmental Agency is responsible for monitoring air, water and soil quality but the General Department of Meteorology is also responsible for monitoring air and water. The Ministry of Agriculture and Rural Development has a mandate to manage water and soil resources and the Ministry of Health has a mandate to oversee sanitary and environmental health issues. This overlap makes governance ineffective.

j) Bureaucratic management mechanism. The environment management practices in Vietnam are guided largely through "Command-and-control' mechanisms instead of market-based or volunteer ones. The government makes the rules for the firms to follow. This practice has some limitations. First, as discussed above, the "Command-and-control" mechanism that is based on fines and punishment does not provide the firms with incentives for investment to reduce negative impacts on environment. Second, due to historical reasons, most assets in Vietnam are still state-owned. This type of ownership does have some advantages in relation to implementing environmental policies because the government is the sole decision makers and there is no need to develop any bargains as is the case with private ownership. However, the absence of the private ownership of assets, together with poor transparency of the administrative system in Vietnam, creates a fertile land for corruption and as a result, the objective of environmental protection is difficult to achieve.

Finally, poor communication and education on environmental issues have also contributed to a poor public awareness and hence emergence of any pressure-constituency on these issues. For example pollution control is generally viewed by the public, including industry, to be a non-productive enterprise, viewed particularly against a backdrop where the performance of the local government officials is judged almost entirely

by how much they are able to increase the region's economic growth. Hence, environmental pollutions and polluters are not of immediate interest to such officials. This also leads to poor cooperation between the environmental monitoring agencies and the polluters.

4. CONCLUSIONS AND RECOMMENDATIONS

The population growth and the government's determination to maintain high rates of economic growth over the next decades will inevitably translate into increased energy demand. Given the modest availability of indigenous energy resources, poor energy infrastructure, and the vulnerability of global sources of energy supply, the security of energy supply is likely to be an issue of utmost importance for the Vietnamese policy makers. Other consequences of rapidly increasing energy demand include increased CO2 emissions and pollution. The existing energy policy framework in Vietnam is characterised by a lack of cohesiveness of policy direction, fragmented institutional structures and responsibilities, and weak public constituency on environmental issues. The existing framework is therefore unlikely to be able to provide a satisfactory redress to the issues noted above. This paper has provided some suggestions about how the weaknesses of the existing framework could be reduced. These include: articulating the significance of the link between energy, economy and environment; developing coherence in institutional purpose and design, and raising public awareness through better communication and education.
The proposals made by this paper, however, are still limited to what should be done to improve the weaknesses of the current policies. Some question, such as how the energy policies should be formulated and to what extent the improving actions should be taken have not been answered. To answer these questions, a comprehensive framework for energy policy analysis is needed. In this framework, not only impacts of the energy options within energy sector are examined but also the economy-wide impacts of those options are investigated. These are outside the scope of this paper and will be done in the future studies.

REFERENCE

[1] IEA. 2007. Energy Balances of Non-OECD Member Countries. *Indicators Vol 2007 Release 01*, http://masetto.sourceoecd.org/vl=2623022/cl=49/nw=1/rpsv/ij/oecdstats/16834240/v285n1/s23/p1

[2] General Statistic Office (GSO), Vietnam. 2008. Value of Exported Goods http://www.gso.gov.vn/default_en.aspx?tabid=472&idmid=3&ItemID=7665

[3] IEA. 2007. Energy Balances of Non-OECD Member Countries. *Energy Balances (ktoe) Vol 2007 release01*, http://masetto.sourceoecd.org/vl=2623022/cl=49/nw=1/rpsv/ij/oecdstats/16834240/v285n1/s19/p1

[4] JICA. 2008. A study on National Energy Master Plan. Appendix 2.1, pp 253.

[5] Ministry of Industry and Trade, Vietnam. 2006. Vietnam Energy Overview and National energy policy. *Draft Report*, http://www.moi.gov.vn/LDocument/

[6] Institute of Energy (IE), Vietnam. 2008. Strategic Plan for New and Renewable Energy Development up to 2015 with vision to 2025. *Final Report, Hanoi*.

[7] Institute of Energy, Vietnam. 2005. Energy Pricing and Its Implication for Energy Efficiency and Environment. *Study Report*, pp 35-32, Hanoi.

[8] Vietnam Electricity (EVN). 2008. EVN should not invest outside power industry to meet national electricity demand. http://vietnamnet.vn/kinhte/2009/02/831891/

[9] APECRC. 2006. APEC Energy Demand and Supply Outlook 2006, http://www.ieej.or.jp/aperc/2006pdf/Outlook2006//ER_Viet_Nam.pdf

[10] IEA. 2007. CO2 Indicators Vol 2007 Release 01, http://masetto.sourceoecd.org.ezproxy.lib.uts.edu.au/vl=3364074/cl=19/nw=1/rpsv/ij/oecdstats/16834291/v335n1/s3/p1

[11] PetroVietnam. 2006. International Cooperation in oil exploration and exploitation. http://www.petrovietnam.com.vn/Modules/PVWebBrowser.asp

[12] Center for European Policy Study. 2004. Market-based Options for Security of Energy Supply. http://www.euractiv.com/en/energy/market-based-options-security-energy-supply/article-128460

[13] World Bank, 2006. Vietnam's electric poer sector: Meeting the challenge of rapid growth, *Final report*, pp 31, Hanoi.

[14] Ministry of Science and Technology. 2006. Environment Management in Vietnam. http://www.most.gov.vn/apec/ENVIRO-VN-9.htm

[15] UNFCCC. 2000. The Kyoto Protocol. http://unfccc.int/kyoto_protocol/items/2830.php

[16] UNFCCC. 2007. Agreement Reached on the Bali Roadmap. http://unfcccbali.org/unfccc/news-unfccc/news-unfccc/agreement-reached-on-the-bali-roadmap.html

[17] Vietnam Registration. 2008. Exhaust Emissions Standards for Road Vehicles.

Program Development Using Dissolved Gas Analysis Method for an Analysis of Power Transformer Oil Testing Results

Thanapong Suwanasri and Cattareeya Suwanasri

Abstract*— *This paper presents a program development for an analysis of power transformer oil testing results. The Dissolved Gas Analysis (DGA) method is applied. This method is generally used to determine transformer condition and failure causes by analyzing quantities of combustible gases in oil. The DGA method consists of three well known methods as the key gases method, the total combustible gases method, and the ratios method. In addition, the failure pattern and reliability of transformer components are analyzed by applying statistic methods as Weibull distribution and Normal distribution methods. Different cases of power transformers were examined in this paper by taking the historical data of power transformers into consideration. Finally, the failure rate and reliability of power transformer components are determined. This program development is designed to be a tool for systematic database management and failure analysis program on web-application to determine the criticality of power transformer components. The strategy and process for preventive maintenance can be built up from causes of failure to improve power transformer as well as system reliabilities.

***Keywords*— Asset management, condition monitoring, dissolved gas analysis, failure statistics, power transformer, preventive maintenance.**

1. INTRODUCTION

Power transformer is one of the important equipment in an electrical power system. Its functions are to transfer an electrical power and change voltage levels. It has high cost and high weight equipment, which is usually used for 20-25 years depending on its life time design [1]. Practically after a new power transformer is operated in an electrical power system, it has been slowly degraded. Abnormal conditions such as overload, lightning strikes, over voltage, harmonics and short circuit events impact significantly to aging of a power transformer until failure occurred. The failures are dangerous for operating personal from firing explosion and others, when severe fault is taken place. In addition, there are environment impacts as oil leakage and supply interruption in a wide area. Those affects on both economics and stability of country. Thus, it is extremely necessary that the power transformer should be provided an appropriate maintenance to maintain availability and reliability in operation [2], [3]. Preventive maintenance on power transformer has been performed following the traditional method using pre-determined time schedule. Transformer testing and maintenance are regularly performed with good knowledge and experiences. However, testing results are scattered and not systematically recorded. This leads to very high cost and long time in service for maintenance because of insufficient and inappropriate data used for condition evaluation. Thus, this following method is setup. At first, the DGA method is selected to evaluate the transformer condition because this method can performed without service interruption and indicated nearly actual condition of transformer because of the up to date result. The scattering failure events are systematically recorded and its database is subsequently setup. Then, the failure analysis is statistically performed to determine the weak component of transformer. Moreover, the expected lifetime of transformer components is determined by using Weibull and Normal distributions for spare part management. The known causes of failure are used to prevent the repeated failure. Next, the web application is applied to grant the remote access of maintenance officer to central data.

2. WORKING PROCEDURE

The working procedure for this paper is as follows. Firstly, the scattering technical data from previous maintenance and historical testing record are obtained and used for database setup and systematic record.

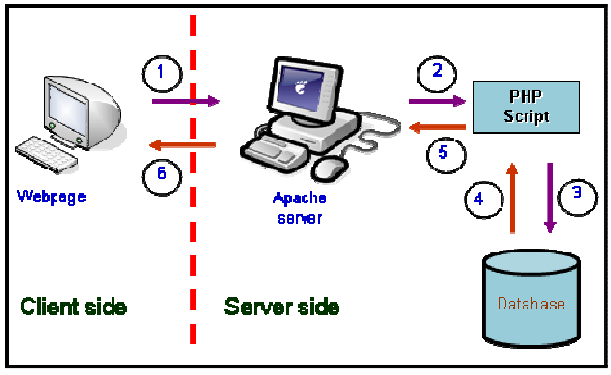

Fig.1. PHP and MySQL for Database Management Program.

Thanapong Suwanasri is with Sirindhorn International Thai – German Graduate School of Engineering, King Mongkut's University of Technology North Bangkok, Bangkok, Thailand.

Cattareeya Suwanasri (corresponding author) is with the Faculty of Engineering, Naresuan University, Phitsanulok, Thailand. Tel: +66-55-961-000 ext. 4342; Fax: +66-55-261-062; E-mail: cattareeyaa@nu.ac.th.

Secondly, webpage is designed for practical and convenient usage. It is performed using web application and relational database. In Fig. 1, the web application design, PHP language, apace server and PhpMyAdmin program is developed for database management.

Thirdly, power transformer models are selected for the study based on the available technical data from maintenance, historical testing record and number of power transformer in service.

Fourthly, the scattering existing data according to region, location, manufacturer and rating and etc are classified. The failure data are divided into major and minor failures by their definitions before recording into the database.

Next, the technical data, which is performed by the analysis of the existing maintenance data for failure statistic and historical testing data for condition evaluation, are analyzed. In data analysis, the percentage of component failure is calculated and condition evaluation is performed by using the Dissolved Gas Analysis (DGA) method [4]-[6]. By this mean, the failure pattern and deterioration trend can be observed and protected. The DGA historical testing results will be interpreted by key gas method [7] and verified by total combustible gas [7], the amount of key gas [7], Dörnenburg and Roger ratio methods [8]. Additional to this step, Weibull and Normal distribution statistical methods are applied to find the failure rate and system reliability caused by each component. Compared to expert system, this program is less complex and suitable for a rough analysis to predict possible problem of transformer. However this program should be subsequently improved by adapting the analysis with the expert system.

Finally, the maintenance activities can be optimally specified from component criticalities, failure causes. Therefore, the aging pattern and trend of the power transformer deterioration can be determined. The result is used to determine the suitable maintenance activities according to component failure, component condition and demand. Moreover, the failure rate of power transformer can be reduced by implementing the preventive measure according to the known causes of failure.

3. BASIC THEORY

3.1 Condition Evaluation by the DGA Technique

The historical testing record has been analyzed by using the DGA. This method is generally used to determine transformer condition by analyzing quantities of combustible gases in oil. The DGA method consists of three well known methods as key gases method, total combustible gases method, and ratios method.

Key Gases Method

The key gas method can basically classify the into four cases abnormal key gas conditions; firstly arcing in oil with acetylene (C_2H_2) as a key gas, secondly corona in oil with hydrogen (H_2) as a key gas; thirdly overheated oil with ethylene (C_2H_4) as a key gas, and lastly overheated cellulose with carbon monoxide (CO) as a key gas.

Total Combustible Gases Method

The total combustible gases method provides the rough estimation of power transformer degradation and abnormal condition by analyzing the amount of gasses from oil testing. For example, if hydrogen in sampled oil is in between 0-500ppm, it indicates satisfactory operation; however, if hydrogen is more than 1000ppm, it indicates corona occurred in power transformer. Similarly, when ethylene in oil shows the value in between 0-20ppm, it is in satisfactory operation; however, when ethylene is more than 150ppm, this means severe overheating happened in the transformer. Other key gases as acetylene and carbon monoxide, when they are found more than 70ppm and 1,000ppm, the transformer faces arcing and severe overheating problems, respectively.

The Ratio Method

The ratio method is separated into two different ratios for transformer oil testing results analysis, which are Dörnenburg ratio method and Rogers ratio method [7], [8]. The Dörnenburg ratio and Rogers ratio methods are used in the analysis. The Dörnenburg ratio indicates three of the four ratios of CH_4/H_2, C_2H_2/C_2CH_4, C_2H_2/CH_4 and C_2H_6/C_2H_2. Therefore, the results will fit into three analysis categories of thermal decomposition, corona with low intensity partial discharge, and arcing with high intensity partial discharge. The Roger ratios indicate the two of the three ratios of C_2H_2/C_2H_4, C_2H_4/H_2, C_2H_4/C_2H_6. The result will fit into four analysis categories as low energy density arcing with partial discharge problem, arcing with high energy density discharge, low temperature thermal, and high temperature thermal.

3.2 Failure Statistic Analysis

Generally, the failure data of power transformer has been presented as event reports. It was usually recorded by preventive maintenance officer of the utilities, consisting of date, time, location, transformer rating, importance failure details and repair/replacement measures. The details of failure are classified into two categories as major/minor failure in order to divide the group of failure data. The major failure is defined as an unplanned service interruption of equipment caused by a lack of one or more fundamental functions with or without supply interruption. This results in a sudden change in system operating conditions and requires non-scheduled repair action [9]. The minor failure is defined as a detection or damage on equipment, which does not lead to a service interruption of equipment. It is not either immediately required a repair action or even could be repaired by a scheduled maintenance measure [9].

In the analysis, life time is defined as the time that product operated successfully or the time that product operated before it failed, measured in hrs, miles etc. Before life data analysis, failure modes and life units such as hrs, miles, cycles etc. must be clearly specified

using a stochastic processes. Similarly, reliability engineering was applied to avoid catastrophic events (loss of life or property). In this paper, Weibull distribution and normal distribution methods are applied.

3.2.1 Weibull Distribution [10]

Weibull distribution is one of the most commonly used distributions in reliability engineering. Procedures for Weibull distribution are data acquisition, ranking data, plotting data on Weibull probability plot and interpreting the result. It provides reasonably accurate failure analysis and failure forecasts with extremely small samples and provides a simple and useful graphical plot. The horizontal scale is the age or time to failure (t). Vertical scale is a cumulative percentage failed or cumulative distribution function (CDF), which is proportion the units that will fail up to age (t) in percent. The Weibull parameters comprise of:

Beta parameter (β) is the shape parameter or the slope of Weibull plot. It indicates class of failure mode. The beta (β) less than 1 indicates decreasing failure rate that is called run-in or burn-in failure period. The beta (β) is equal 1, which indicates constant failure rate. This period is called design life or random failure period. The beta (β) more than 1 indicates an increasing failure rate, which is called wear out period.

Eta parameter (η) is Weibull characteristic life. It is measure of the scale or spread in the distribution of data. The eta (η) parameter is equal to the time at 63.2 percent of the unit has failed. In the other words, the eta (η) is equal to the time at 36.8 percent surviving units or reliability is equal 0.316.

Gamma parameter (γ) is the location parameter utilized when the data do not fall on a straight line, but fall on either a concave up or down curve. It is location of the origin of a distribution (time shift) and provided an estimation of the earliest time-to-failure. Period between 0 and γ is failure free time.

Weibull Statistical Properties

- Probability distribution function (PDF)

$$f(t)=\left(\frac{\beta}{\eta}\right)\left(\frac{t-\gamma}{\eta}\right)^{\beta-1} e^{-\left(\frac{t-\gamma}{\eta}\right)^{\beta}}, t \geq \gamma \quad (1)$$

- Cumulative distribution function (CDF)

$$F(t)=1-e^{-\left(\frac{t-\gamma}{\eta}\right)^{\beta}} \quad (2)$$

- Reliability (R(t))

$$R(t)=1-F(t)=e^{-\left(\frac{t-\gamma}{\eta}\right)^{\beta}} \quad (3)$$

- Failure rate (λ(t))

$$\lambda(t)=\frac{f(T)}{R(t)}=\left(\frac{\beta}{\eta}\right)\left(\frac{t-\gamma}{\eta}\right)^{\beta-1} \quad (4)$$

3.2.2 Normal Distribution

Maximum Likelihood Estimation (MLE)

Two quantities have been specified for the normal distribution, which are mean value (μ) and standard deviation (σ).

- Mean value (μ)

$$\mu=\frac{\sum_{i=1}^{n} t_i}{N} \quad (5)$$

- Standard deviation (σ)

$$\sigma=\sqrt{\frac{\sum_{i=1}^{n}(t_i-\mu^2)}{N-1}} \quad (6)$$

Normal Statistical Properties

- Probability distribution function (PDF)

$$f(t)=\frac{1}{\sigma\sqrt{2\pi}} e^{-\frac{1}{2}\left(\frac{t-\mu}{\sigma}\right)^2} \quad (7)$$

- Cumulative distribution function (CDF)

$$F(t)=\int_0^t \frac{1}{\sigma\sqrt{2\pi}} e^{-\frac{1}{2}\left(\frac{t-\mu}{\sigma}\right)^2} \quad (8)$$

- Reliability (R(t))

$$R(t)=1-F(t) \quad (9)$$

- Failure rate (λ(t))

$$\lambda(t)=\frac{f(t)}{R(t)} \quad (10)$$

4. RESULTS

4.1 Condition Evaluation by DGA Technique Results

The condition evaluation of power transformer was studied by considering the scattering historical data of power transformers but only one example unit of power transformer was presented in this work. The oil testing record is analyzed.

The Sample Transformer

A transformer is of rated 115/22kV, 25MVA. The transformer oil was sampled in July 28, 1982 and tested in July 28, 1982. The DGA testing results are shown in Table 1. The data is analyzed from the methods in

Section 3.1.

Table 1. DGA Testing Result in July 28, 1982 of a Rated 115/22kV, 25MVA Transformer

GAS	CO	H_2	CH_4	C_2H_6	C_2H_4	C_2H_2
VALUE	273	403	0	113	109	212

- *Key Gas Method*

From the data, it is analyzed and plotted as in Fig. 2. Acetylene (C_2H_2) is key gas with large amount of hydrogen and acetylene, which indicates the problem involving the arcing in oil.

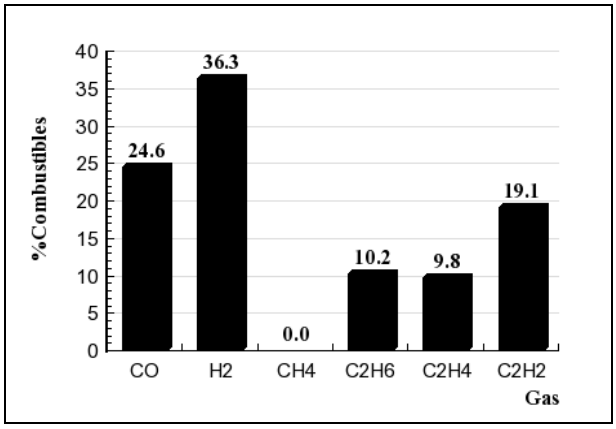

Fig.2. Percentage of Combustible Key Gases for Arcing in Oil Problem.

- *Total Combustible Gases Method*

The total combustible gases method provides the rough estimation of power transformer degradation. Fig. 3 shows the amount of total combustible gases, which reaches 1199 ppm in July 28, 1982.

This indicates the significant decomposition and the increasing trend should be carefully observed. If the amount of combustible gases remains constant, the decomposition process is stopped due to the self-healing effect. If the amount increases, then the unit can be in the danger zone.

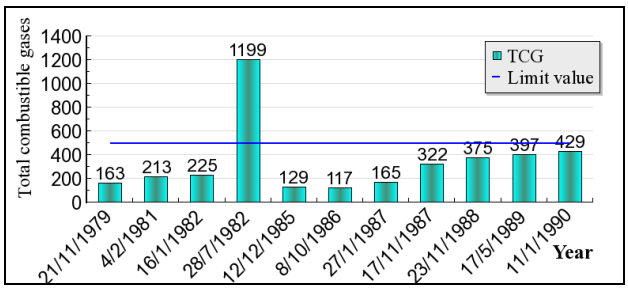

Fig.3. Relationship Between the Total Combustible Gases and Age.

From the DGA historical testing results each year, the trend of generating combustible gases is presented in Fig. 4. The increasing trend of combustible gases relative to service year of power transformer can be determined. Each combustible gas indicates the cause and severity of the problem.

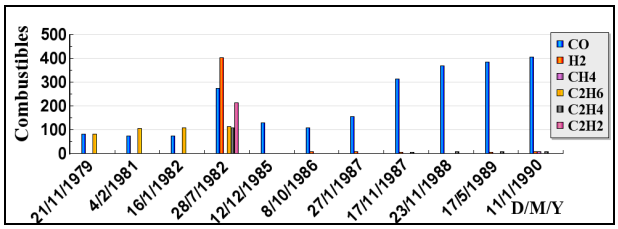

Fig.4. Relationship between Key Combustible Gases and Age.

- *Ratios Method*

The Dörnenburg ratio and Rogers ratio method are used in the analysis. The calculation of gas ratios in Table 2 and Table 3 are compared with the reference table for result interpretation. Dörnenburg ratio method indicates three of the four ratios, CH_4/H_2, C_2H_2/CH_4, and C_2H_6/C_2H_2, which fit in the category of corona (low intensity PD). Rogers Ratio Method indicates two of the three ratios, CH_4/H_2 and C_2H_4/C_2H_6, which fit in the category of low-energy density arcing-PD.

Table 2. Dörnenburg Ratio Result

DOERNENBURG RATIO METHOD APPLIED TO HISTORICAL CASES			
R1 (CH_4/H_2)	R2 (C_2H_2/C_2H_4)	R3 (C_2H_2/CH_4)	R4 (C_2H_6/C_2H_2)
0	1.94	0	0.53

Table 3. Rogers Ratio Result

ROGERS RATIO METHOD APPLIED TO HISTORICAL CASES		
R1(CH_4/H_2)	R2(C_2H_2/C_2H_4)	R5(C_2H_4/C_2H_6)
0	1.94	0.96

These analytical results are partly verified, when it is possible to untank the transformer for internal inspection. The accuracy of this analysis is now examining with the possible cases.

4.2 Failure Statistic Analysis Results

The applied power transformers consist of two sample models of 107 units of rated 115/22kV and 44 units of Rated 230/115/22kV are studied. The failure statistics consists of 157 failure events for 115/22kV and 63 failure events for 230/115/22kV power transformer respectively. The data are compared with the failure statistics according to Cigré [11].

Failure Statistics According to Cigré

According to [11], the group of power transformer components can be divided into, on/off-load tap-changer, leakage concerning tank and insulating fluid, bushing, winding, core, and others such as temperature problem. The failure of power transformer as reported in [11] is presented in Fig. 5.

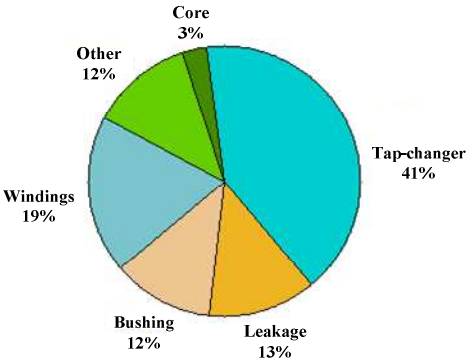

Fig. 5. Failure Statistics of Power Transformer Components Reported by Cigré [11].

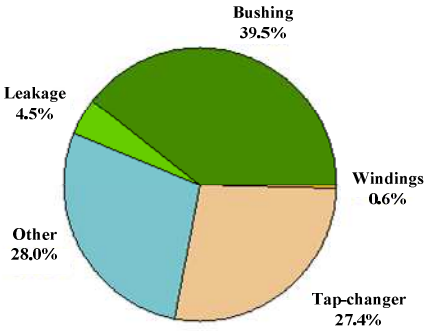

Fig. 6. Failure Statistics of Power Transformer Components for 115/22kV Power Transformer.

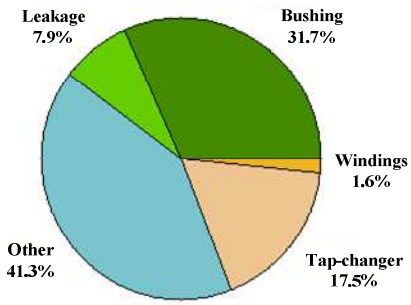

Fig. 7. Failure Statistics of Power Transformer Components for 230/115/22kV Power Transformer.

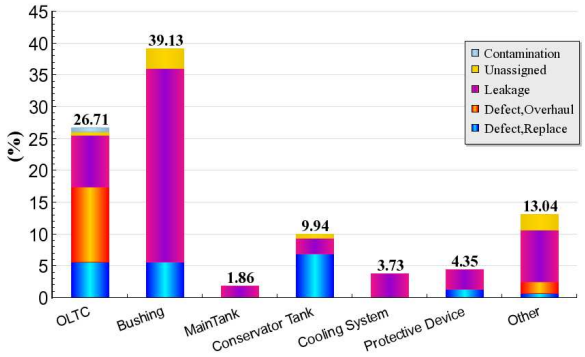

Fig. 8. Percentage of Component Failures and Their Associated Causes for 115/22kV Power Transformer.

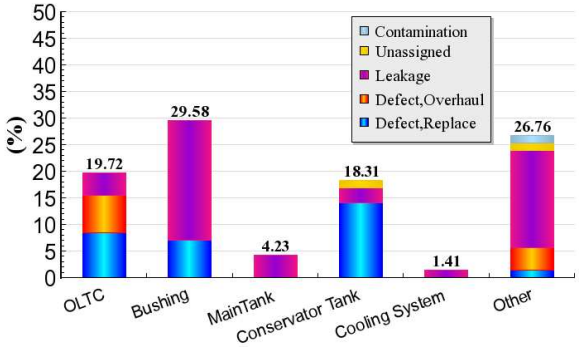

Fig. 9. Percentage of Component Failures and Their Associated Causes for 230/115/22kV Power Transformer.

Failure Statistics of Adopted Power Transformers

By dividing the failure data in the similar categories as above, the failure statistics of adopted power transformer models can be presented in Fig. 6 and Fig. 7. The failure results show the similar contribution of component failure. The critical components of both power transformer types with the highest failures are bushing and tap changer respectively.

Critical Components and Failure Causes

The percentage of component failures and their associated causes are shown in Fig. 8 for 115/22kV power transformer. From the total 158 minor failures of 107 transformer units, the components with high percentage of failure are bushing 39.13% and OLTC 26.71%. The major causes of failure are leakage for bushing, and defect and leakage for tap changer. Fig. 9 shows the percentage of component failures and their associated causes of 230/115/22kV power transformer. From the total 68 minor failures of 44 transformer units, the components with high percentage of failure are bushing 29.58% and OLTC 19.72%. The major causes of failure are leakage for bushing, and defect for tap changer.

Life Time Estimation of Power Transformer Components

For life estimation, three models of power transformers are performed as follows; 115/222kV with 25MVA and 50MVA as well as 230kV/115kV 200MVA, based on the available technical data, historical testing record and numbers in service of 53, 49 and 28 units, respectively.

The failure components, causes and results of Weibull parameters' calculation are presented in the Table 4. From data, the failure analysis is further calculated.

However, because of limitation of paper, only a tank for 115/22kV, 25MVA transformer is shown as an exemplar. The probability density function, reliability, and failure rate for tank leakage are presented in Fig. 10 to Fig. 12, respectively.

In Fig. 10, the PDF curve shows the probability density failure of tanks, which mostly fail in the age about 20 years. This because of all existing data, the age is in average of 20 years. Fig. 11 and Fig.12 show that the failure rate of the tank keeps increasing with the age; by contrast the reliability of the tank keeps reducing. As a result, the component needs to be often focused when it is operated for such a period in order to avoid any severe fault.

Table 4. Life Time Estimation by Weibull Distribution

Component	Failure causes	Rating	Weibull parameters		MTBF
			β	η	
Load Tap Changer	damage	115/22kV, 25MVA	2.92	14.83	13.23
Load Tap Changer	leakage	115/22kV, 25MVA	1.98	17.61	15.61
Bushing	leakage	115/22kV, 25MVA	2.29	24.94	22.09
Tank	leakage	115/22kV, 25MVA	2.97	22.02	19.66
Tank	leakage	115/22kV, 5MVA	3.55	16.11	14.51
Tank	leakage	115/22kV, 200MVA	2.78	22.65	20.16
Bushing	leakage	230/115kV, 200MVA	3.99	18.82	17.06

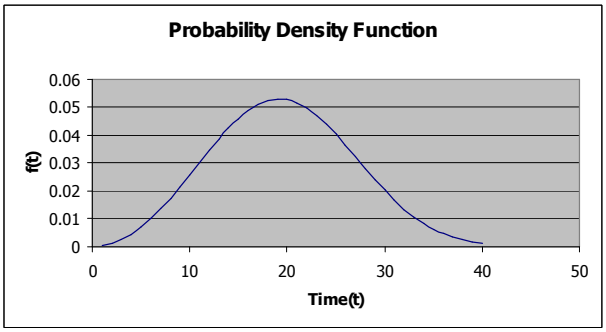

Fig. 10. Probability Density Function for Tank Leakage of 115/22kV, 25MVA Power Transformer.

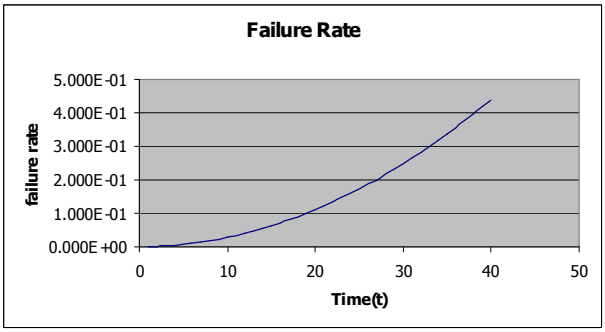

Fig. 11. Failure Rate for Tank Leakage of 115/22kV, 25MVA Power Transformer.

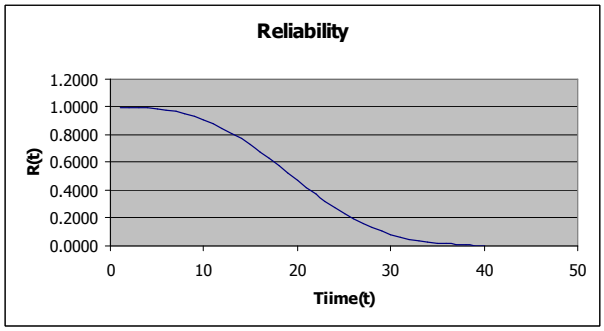

Fig. 12. Reliability for Tank Leakage of 115/22kV, 25MVA Power Transformer.

Because, the calculation result, such as percentage of component failure, its associated causes, estimated of component lifetime, MTBF, failure rate, reliability of components, are based on statistical method, the reliable result could be obtained from the reasonable number of event records and trustable data. Thus, after obtaining more and more such a good input data, the result should be more reliable.

5. CONCLUSION

The scattering historical data of power transformers was managed in a systematic database and analyzed by using developed program in the designed web-application. The different cases of power transformers were examined. The oil testing analysis was performed by applying the dissolved gas analysis in order to evaluate power transformer conditions such as normal or abnormal operating conditions. By the way, the statistic methods as the Weibull distribution and normal distribution were applied to historical failure record in order to obtain the failure rate and reliability of the transformer components. Because this program development offers data pooling, remote access by web application with user friendly interface, simple to use and allowing for further development, it is very useful for maintenance management. From the determination of the critical power transformer components and its associated causes, the strategy and process for preventive maintenance can be effectively set up. The critical components can be carefully maintained. The known causes of failure can help to avoid repeated failure and improve the transformer and system reliability. The procedure in this work can be further adapted to the other equipment in power system.

ACKNOWLEDGMENT

The authors gratefully acknowledge the contributions of the Power Transformer Maintenance Department and Center of Excellence for Transmission System Technology, EGAT, Thailand, for providing the data, close co-operation and strong support for this work.

REFERENCES

[1] Arshad, M., Islam, S.M., and Khaliq, A. 2004. Power transformer insulation response and risk

assessment. *Probabilistic Methods Applied to Power Systems*, 12-16 Sept., pp. 502-505.

[2] Wang, M., Vandermaar, A.J., and Srivastava, K.D. 2002. Review of condition assessment of power transformer in service. *Electrical Insulation Magazine*, IEEE, pp. 12-15.

[3] Arshad, M., Islam, S.M. 2004. Power transformer aging and life extension. *Probabilistic Methods Applied to Power System*, 12-16 Sept., pp. 498-501.

[4] Bandyopadhyay, M.M. 2005. A review on transformer diagnostics. In *Proceedings of the 37th Annual North American Power Symposium*, IEEE. 23-25 Oct., pp. 304-309.

[5] Saha, T.K. 2003. Review of modern diagnostic techniques for assessing insulation condition in aged transformers. *Dielectrics and Electrical Insulation*, IEEE. Oct., pp. 903-917.

[6] Setayeshmehr, A., Akbari, A., Borsi, H., and Gockenbach, E. 2004. A Procedure for diagnosis and condition based maintenance. In *the Proceedings on the IEEE International Symposium on Electrical Insulation.* 19-22 Sept., pp. 504-507.

[7] IEEE guide for the interpretation of gases generated in oil-immersed transformers, IEEE Standard C57.104-1991, July 1992.

[8] Myers, S.D., Kelly, J.J., and Parrish, R.H. 1981. A Guide to Transformer Maintenance. United Stated of America: S.D. Myers Inc., pp. 323

[9] Stafan, F. 2007. Data Management and Case Studies. In *Proceedings of the Asset Management Workshop*. Bangkok Thailand.

[10] Aberneth B.R. 2004. *The New Weibull Handbook: Reliability and Statistical Analysis for Predicting Life, Safety, Survivability, Risk, Cost and Warranty Claims*. 5th Edition.

[11] Jongen, R.A., Morshuis, P.H.F. Smith, J.J., Janssen, A.L.J., and Gulski, E. 2007. Failure data of power transformers as input for statistical failure analysis. In *Proceeding of the 15th International Conference on High Voltage Engineering*, Slovenia.

Stochastic Voltage Sag Prediction in Distribution System by Monte Carlo Simulation and PSCAD/EMTDC

T. Meananeatra and S. Sirisumrannukul

***Abstract*— *Voltage sag is defined as a temporary rms reduction in voltage typically lasting from a half cycle to several seconds. Voltage sag may produce unfavorable consequence in production processes if the process-control equipment trips. Therefore, analysis of voltage sags at a location of interest provides useful information for assessing the compatibility between equipment and the electrical supply. As the primary cause of voltage sag is due to faults that may occur anywhere in distribution systems, a Monte Carlo simulation method is proposed as the main tool for voltage sag prediction in this paper. The Monte Carlo simulation method is employed to capture stochastic behavior of fault consisting of fault location, initial time of fault, fault duration and fault type. PSCAD/EMTDC, which is a software package developed to simulate electric-magnetic transient phenomena, calculates voltage sag magnitude and duration. Power flow solution is obtained from the software PSS/E and used by the E-TRAN program to directly initialize the circuit in PSCAD/EMTDC. A distribution system of Metropolitan Electricity Authority (MEA) is tested in a case study. With the proposed methodology, the expected value of voltage sag magnitude and their probability distribution can be obtained. This information is useful for the utility and customers for voltage sag prevention.*

***Keywords*— Monte Carlo simulation, PSCAD/EMTDC, sag duration, sag magnitude, voltage sag.**

1. INTRODUCTION

A variety of power quality problems exists in distribution systems but voltage sag is probably the most prominent one due to the fact that temporary faults are most often seen. Voltage sag is a temporary root mean square (rms) drop in voltage magnitude ranging from 0.1 per unit and 0.9 per unit of the nominal voltage and sag duration is one half cycle to one minute [1].

The problem of voltage sags is gaining importance because they affect industrial and large commercial customers whose production processes can be disrupted as a result of tripping of their sensitivity equipment such as adjustable speed drive, computers and computer-controlled equipment. The consequence of voltage sags may produce high economic loss of productivity.

The primary cause of voltage sag is due to faults that may occur anywhere in a system and cannot be eliminated completely. There are a number of factors associated with voltage sag such as location, the characteristics of utility's distribution system (underground, overhead, lengths of the distribution feeder circuits, and number of feeders), number of trees adjacent to the power lines, and several other factors [2].

This paper presents a methodology for predicting voltage sags characteristics caused by faults in a distribution system. Predicting voltage sag requires a tool that can provide information for the utility to identify the weak points or locations and to assist the utility' customers to select appropriate equipment specifications to assure the optimum operation of their production facilities [3].

A Monte Carlo simulation is proposed for voltage sag prediction in which time domain analysis is carried out using the PSCAD/EMTDC software package interfaced with PSS/E and MATLAB programs. The advantage of the proposed method is that the stochastic nature of faults can be statically captured with minor mathematical calculation involved. With our method, prefault voltage, a variety of fault types, sag magnitude, and sag duration can be taken into account. The developed tool is tested with a distribution system of Metropolitan Electricity Authority (MEA).

2. STOCHASTIC VOLTAGE SAG PREDICTION

There are basically two major methods for voltages sag assessment: analytical and simulation methods. Analytical methods, such as fault position [4], represent the system by analytical model and evaluate system indices using mathematical solutions. The Monte Carlo simulation method, on the other hand, estimates the system indices by simulating the actual process and random behavior of the system [5]. The analytical method is superior to the Monte Carlo simulation method in computation time because the Monte Carlo simulation method is normally computationally expensive to arrive at results with sufficient confidence. However, for systems with complex operating conditions or those in which parameters cannot be explicitly modeled, Monte Carlo methods are preferable.

Monte Carlo simulation mimics system behaviors and estimates system parameters by simulating the actual process. It does not solve the equations describing the model; instead the stochastic behavior of the model is

T. Meananeatra (corresponding author) is with Better Care and Power Quality Department, Metropolitan Electricity Authority 132/18, Soi Charansanitwong 20, Charansanitwong Rd., Banchanlor, Bangkoknoi, Bangkok, 10700, Thailand. Phone: +66-2878-5297; E-mail: tanit.m@mea.or.th.

S. Sirisumrannukul is with the Department of Electrical Engineering, Faculty of Engineering, King Mongkut's University of Technology North Bangkok, 1518, Pibulsongkram Rd., Bangsue, Bangkok, 10800, Thailand. Email: spss@kmutnb.ac.th.

simulated and observed for several iterations [6]. The simulation process is repeated until the solutions converge. The convergence can be confirmed when no significant variation in the solution is observed or the prespecified number of iterations has been reached. Monte Carlo simulation generally requires considerable computation time in order to obtain sufficient confidence in the results [7]. Alternatively, for the sake of computation time reduction without losing confidence in the accuracy of the results, a number of techniques based on variance reduction were developed and often employed, such as importance sampling, stratification, control variates and antithetic variates.

Every time the system is run, several quantities are randomly generated to represent fault characteristics whose probability distributions are normally predefined based on statistical behavior of fault. Two factors that describe voltage sag characteristic are sag magnitude and sag duration. Figure 1 shows a sag produced by a single line to ground fault at phase C in the test system detailed in Section 5. With this waveform, the sag occurs at phase C, while the voltages at phases A and B remain unchanged. The sag magnitude is 0.193 pu. with a duration of 71.2 milliseconds.

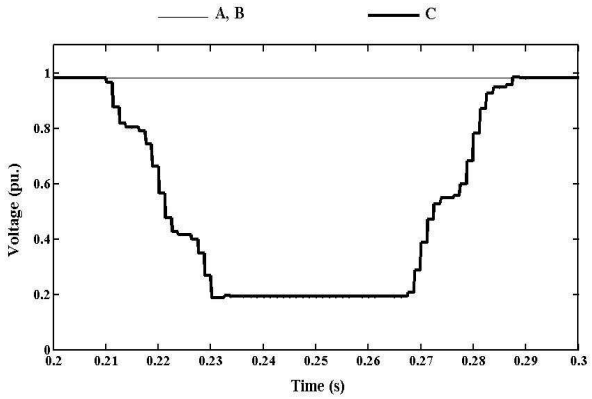

Fig.1. Voltage Sag Waveform.

In the process of Monte Carlo simulation, four parameters need to be randomly generated as follows.

a) Fault locations can be modeled by the method of fault position [8]. The main concept behind this method is that a fault can be originated from every single position on a distribution line (sending and receiving end buses are considered as points on the line). However, taking into consideration of all the points on the line, although possible, is time-consuming. Thus, a distribution line with equally divided intervals, say four segments as shown in Fig. 2, would be reasonably approximated. This approximation introduces three dummy buses between bus 1 and bus 2. Therefore, there are five possible locations exposed to faults.

The parameters associated with a probability distribution of fault position can be determined from past experience. However, without historical data, a density function for fault location can be based on the uniform density function. A fault location is mathematically expressed by (1).

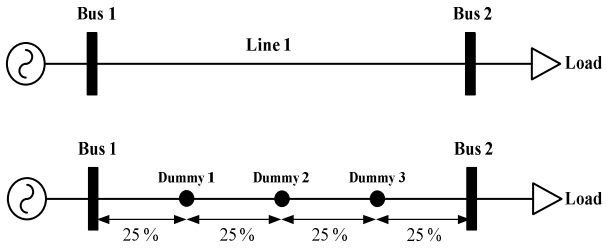

Fig.2. Method of Fault Position.

$$FL_i = \begin{cases} i = 1, & \text{if } 0 < U_1 \le 1 \\ i = 2, & \text{if } \frac{1}{n} < U_1 \le \frac{2}{n} \\ \quad \bullet & \\ \quad \bullet & \\ \quad \bullet & \\ i = n-1, & \text{if } \frac{n-2}{n} < U_1 \le \frac{n-1}{n} \\ i = n, & \text{if } \frac{n-1}{n} < U_1 \le 1 \end{cases} \quad (1)$$

where i = bus index
n = total bus number
U_1 = uniform random number under [0,1]

b) The initial time of a fault is represented by a random number that is uniformly distributed within 1 cycle (50 Hz or 20 milliseconds).

$$FI = U_2, \quad \text{if } 0 < U_2 \le 0.02 \quad (2)$$

where FI = initial time of the fault
U_2 = uniform random number under [0,0.02]

c) The fault duration of voltage sag is assumed to be normally distributed with a mean and a standard deviation. For a given uniform random number under [0, 1], it can be converted to a normally distributed random number by an approximate inverse transform method [7].

$$X = \begin{cases} z, & \text{if } 0.5 < U_3 \le 1.0 \\ 0, & \text{if } U_3 = 0.5 \\ -z, & \text{if } 0 < U_3 < 0.5 \end{cases} \quad (3)$$

$$FD = (X \times \sigma) + \mu \quad (4)$$

where z = random variable calculated using the equations given in the appendix
U_3 = uniform random number under [0,1]
X = normally distributed random variants
μ = mean of fault duration
σ = standard deviation of fault duration
FD = fault duration

d) Fault types are classified as three-phase fault, double line-to-ground fault, line-to-line fault and single-line-ground fault. A probability distribution of fault type can be modeled by a discrete distribution derived in (5).

$$FT_j = \begin{cases} j=1, & \text{if } U_4 \le P_{LLL} \\ j=2, & \text{if } P_{LLL} < U_4 \le (P_{LLL} + P_{LLG}) \\ j=3, & \text{if } (P_{LLL} + P_{LLG}) < U_4 \le (P_{LLL} + P_{LLG} + P_{LL}) \\ j=4, & \text{if } (P_{LLL} + P_{LLG} + P_{LL}) < U_4 \le 1 \end{cases} \quad (5)$$

where j = fault index
FT_j = fault type
U_4 = uniform random number under [0, 1]
P_{LLL} = probability of occurrence of a three-phase fault
P_{LLG} = probability of occurrence of a double line-to-ground fault
P_{LL} = probability of occurrence of a line-to-line fault
P_{LG} = probability of occurrence of a line-to-ground fault

In practice, the values of the four probabilities can be determined from statistical collected data.

After bus voltages have been calculated, the expected bus voltage magnitude is given by the following equation:

$$\overline{V_j} = \frac{1}{N}\sum_{k=1}^{N} V_k \quad (5)$$

where $\overline{V_j}$ = expected value of sag magnitude at bus j
V_k = sag magnitude of iteration k
N = number of samples

The unbiased sample standard deviation for bus voltage magnitude is calculated from:

$$\sigma_j = \sqrt{\frac{1}{N-1}\sum_{k=1}^{N}\left(V_k - \overline{V_j}\right)} \quad (7)$$

where σ_j = sample standard deviation

Note that according to IEEE Std 493-1997 [9], V_k in (6) is considered from the lowest of three phase voltages for each sag event.

3. DEVELOPED SIMULATION TOOL

Power System Computer Aided Design (PSCAD)/ Electromagnetic Transients including DC (EMTDC) [9] is a fast, accurate, and user-friendly power system simulation software. The software is suitable for time domain simulation, particularly in transient periods. It contains extensive libraries of power and control system models organized in forms of circuit schematic. A user can construct a circuit, run a simulation, analyze the results, and manage data in graphical environment.

Although PSCAD/EMTDC offers a convenient way for voltage sag simulation, it still needs an interface with external subroutines that is able to perform special tasks. The proposed simulation tool links the multiple run option in PSCAD/EMTDC with PSS/E for calculating power flow solutions and with a module developed on MATLAB for data recording and post processing of output results. Figure 3 shows a flowchart of proposed stochastic simulation tool for voltage sag prediction. The duration of each run performed by PSCAD/EMTDC is 0.5 second with a time step of 0.1 milliseconds.

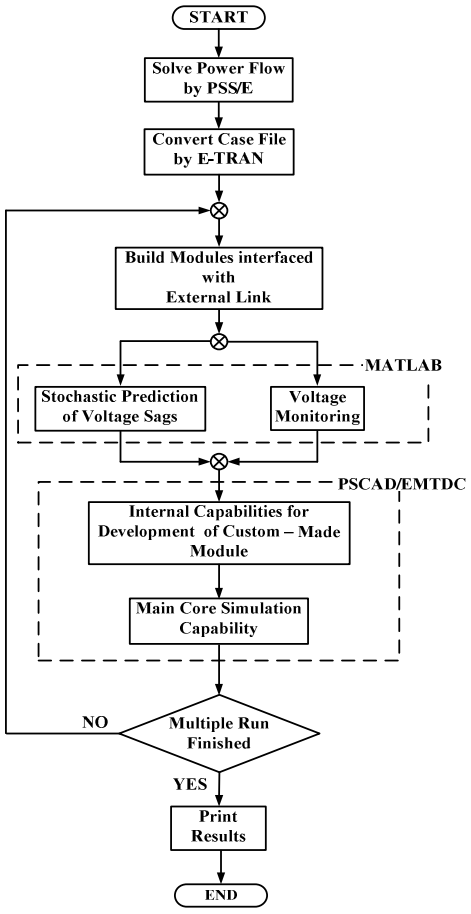

Fig.3. Developed Simulation Tool for Voltage Sag Prediction.

4. METHODOLOGY FOR VOLTAGE SAG ASSESSMENT

The proposed methodology consists of following steps.

Step 1: Input data of loads, branches, buses, network equivalent of supply point and maximum number of iterations.

Step 2: Perform power flow by a subroutine in the PSS/E program to obtain pre-fault bus voltages (including those at dummy buses). The PSS/E program gives a case file that contains all the input data and the power flow solution.

Step 3: Convert the case file by the E-TRAN program, which directly initializes the circuit in PSCAD/EMTDC.

Step 4: Interface PSCAD/EMTDC with MATLAB by a custom-made module for a Monte Carlo simulation and for data recording.

Step 5: Generate random numbers by a subrountine in MATLAB to represent fault characteristics (fault location, initial time of fault, fault duration, fault type). These random number will be used in PSCAD.

Step 6: Perform an electromagnetic transient simulation by PSCAD/EMTDC to obtain sag magnitude and sag duration of all the buses until the maximum iteration has been reached. These two parameters as well as the fault characteristics will be passed to MATLAB for recording.

Step 7: Manipulate the recorded data to obtain the expected voltage sag magnitude and its density function of each bus.

5. CASE STUDY: BANG–PU INDUSTRIAL ESTATE

Description of test system

The 115/24kV Praekasa (PR) distribution substation of MEA is selected for demonstrating a practical case study. The substation is located in the Bang–Pu Industrial Estate of Samutprakan province and supplies 3 power transformers, serving 33 load points with a total demand of 28.5 MW. There are 4 outgoing 24 kV feeders from power transformer No.3, namely PR432 with 2.46 circuit-km, PR434 with 39.4 circuit-km, PR435 with 8.90 circuit-km, and PR433 with 1.45 circuit-km. This system is of interest because it has experienced a number of sags that caused interruption to customers' production processes. The single line diagram of the system is shown in Figure 4. As described in Section 2 for the modeling for fault position, this system has 129 dummy buses in total for the Monte Carlo simulation. The mean and standard deviation for fault duration are 0.06 second and 0.01second [11], [12]. The values used in fault type simulation are $P_{LG} = 0.80$, $P_{LLG} = 0.17$, $P_{LL} = 0.02$, $P_{LLL} = 0.01$ and [11]. It is assumed that fault resistance is neglected.

Simulation Results

The test system is simulated by a multiple run of 500 iterations. The frequency distribution with 10 bins of fault location and initial time of fault is shown in Figures 5 and 6. It is seen that both figures follow the prespecified uniform distribution. As shown in Figure 7, the distribution of fault duration has a mean value of 0.0610 second and a standard deviation of 0.0108 second. These values follow the predefined statistical property of fault duration. As expected from Figure 8, the probability of simulated fault type has a good agreement with the given assumption of fault type; that is $P_{LG} = 0.744$, $P_{LLG} = 0.20$, $P_{LL} = 0.038$, $P_{LLL} = 0.018$.

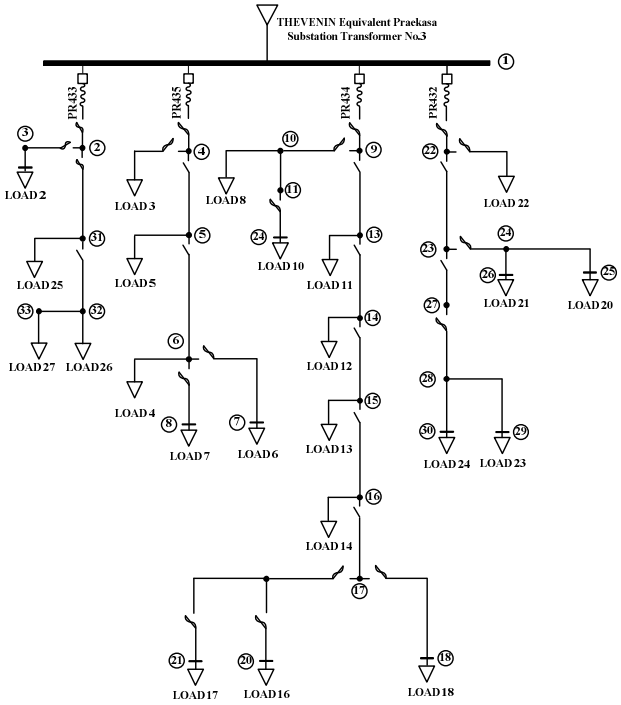

Fig.4. 115/24kV Praekasa Distribution System.

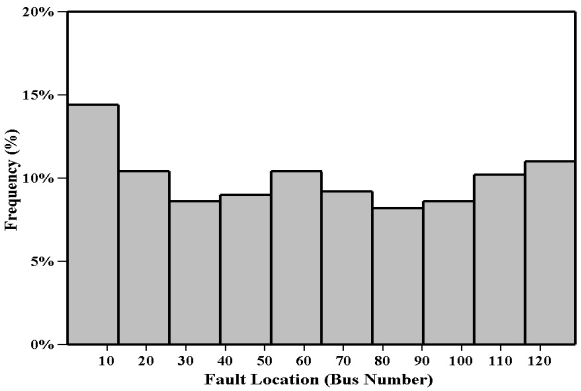

Fig. 5. Density Functions of Fault Location.

Figure 9 shows the density functions of 4 selected buses of interest: bus 9, bus 8, bus 21 and bus 30. It is obviously seen from the figure that bus 9 has the highest average bus voltage while that of bus 21 is lowest. This is not surprising because bus 9 is close to the substation, while bus 21 is at the end of feeder PR434, which is the longest feeder. Downstream customers, of course, tend to suffer more from voltage sags than those upstream. The reason is that a downstream fault may not create a sag seen by upstream customers but downstream customers will certainly be affected by an upstream fault.

Figure 10 illustrates a convergence report of the bus voltages. It is observed that the simulation converges after 300 iterations. The cumulative voltage sag density function of bus 9 is depicted in Figure 11, indicating for example that if a device can ride-through short duration sag, say above 70% of the nominal voltage within 0.1 second, there is a 80% chance that the device will be tripped.

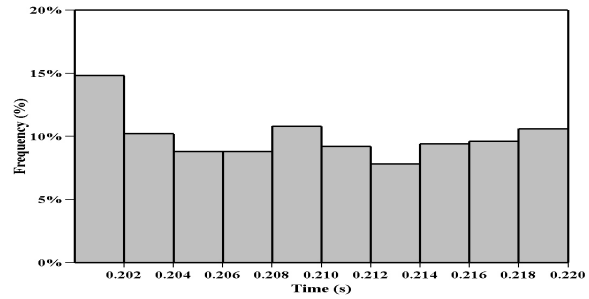

Fig.6. Density Function of Initial Time of Fault

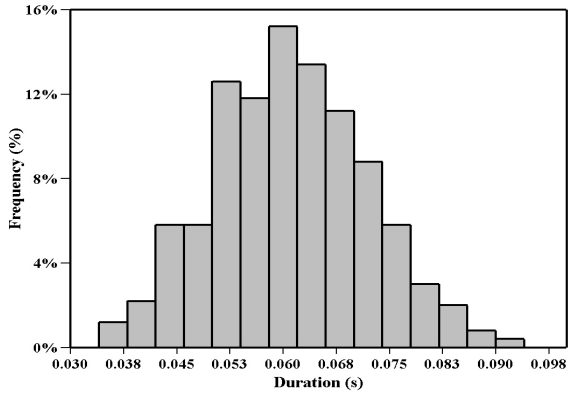

Fig.7. Density Function of Fault Duration.

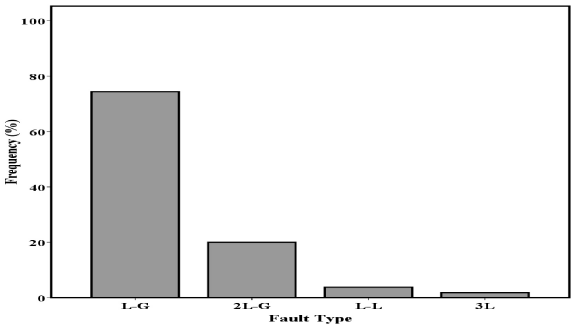

Fig.8. Density Functions of Fault Type.

The developed program takes 36 hours on PC Pentium M 1.6 GHz with 1GB of RAM. The major contribution to the computation time is the number of nodes (or buses) and sampling period (solution time step) being considered. To be specific, the more nodes (buses) or smaller sampling periods, the more computation time. Our problem has in total 129 nodes with a sampling period of 0.0001 sec. It was recommended in [13] that a time step size be equal to or greater than 100 μs (0.0001 sec). The computation time is greatly reduced if we do an analysis only at a bus of interest. As an illustration, it takes only 1.5 hours if only bus 21 is selected in our calculation. Alternatively, if a sampling period is changed from 0.0001 sec to 0.0004 sec with the same 129 nodes, the computation time is only about 9.5 hours, scarifying very small amount of accuracy. Figure 12 emphasizes our confirmation. Nonetheless, computation time does not matter as voltage sag assessment is not for real-time application but rather for planning objective.

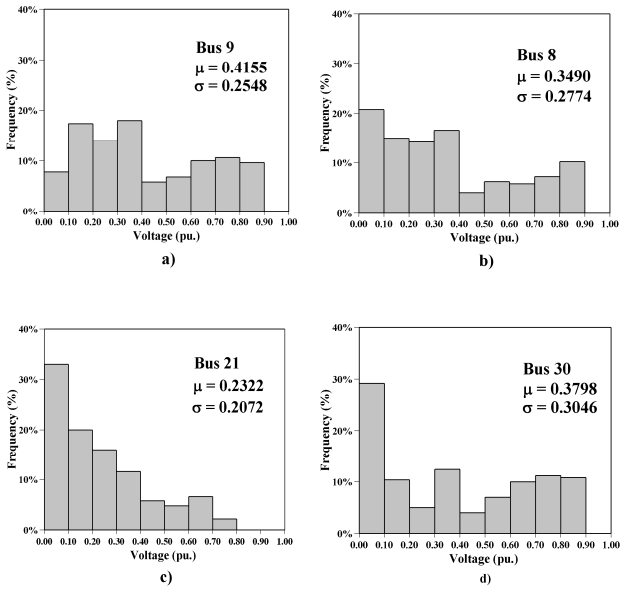

Fig.9. Density Functions of Voltage Sag Magnitudes at 4 Buses.

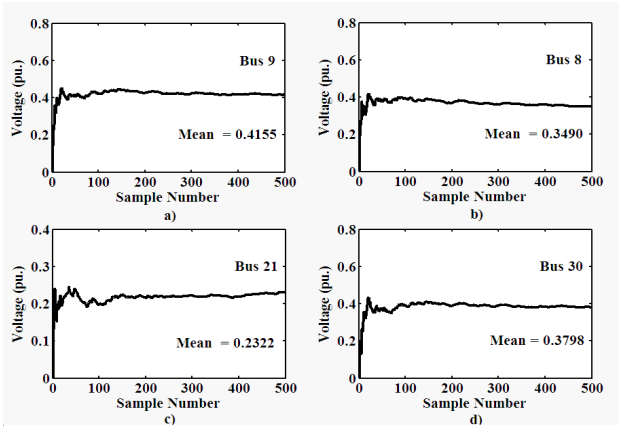

Fig.10. Convergence of Expected Voltage Sag Magnitudes at 4 Buses with sampling period of 0.0001 sec.

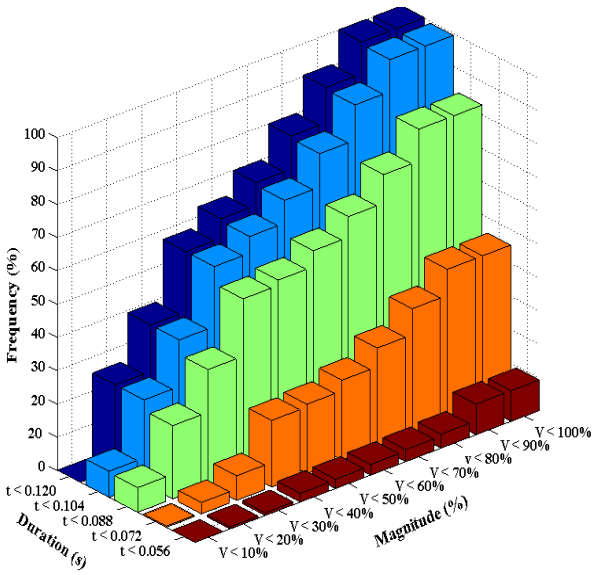

Fig.11. Voltage Sag Distribution Function at Bus 9.

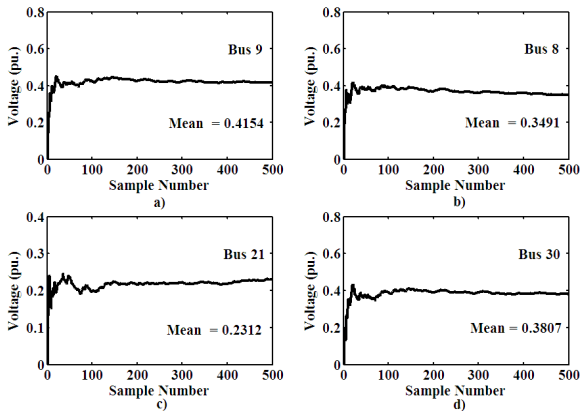

Fig.12. Convergence of Expected Voltage Sag Magnitudes at 4 Buses with sampling period of 0.0004 sec.

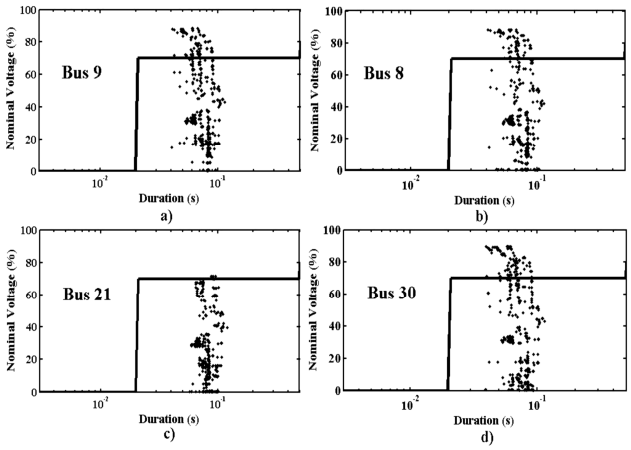

Fig.13. Scatter Diagram of 4 Buses with ITIC Curve.

Figure 13 shows a scatter diagram of sag magnitude versus semi-logarithmic duration for the 4 buses, plotted on a part of the so called ITIC (Information Technology Institute Council) curve [14]. This curve is a loci drawn that establishes a criterion of the tolerance voltages of variations. Any point above the line has a ride-through capability for voltage sags. It is very interesting to note that although the expected voltage at buses 8, 9, 21 and 30 is below 70%, some sag events do not cause problems on the equipment connected to these buses.

6. CONCLUSION

A Monte Carlo based simulation of voltage sags has been presented in this paper. A time-domain simulation tool that integrates the PSCAD/EMTDC software package with PSS/E and MATLAB was developed to estimate voltage sag characteristics quantified by their magnitude and duration. The proposed methodology is demonstrated by a distribution system of MEA. The obtained results are statistically analyzed to give average bus voltages and their density functions. The case study reveals that voltage sag problems are location-specific. Downstream customers are more subject to voltage sag than those upstream because the distribution system under study is radially operated. Scatter diagrams on the ITIC curve is also presented which provides a useful indicator for voltage sag problems. From the utility point of view, voltage sags can be mitigated by fault prevention activities and modification of fault clearing practices, while from the customers' point of view, installing mitigating equipment such as uninterruptible power supply and voltage source converter could be a good option for improving the immunity of sensitive equipment.

ACKNOWLEDGMENT

The first author would like to express his sincere thanks to Research and Development Department, Power System Control Department, and Better Care and Power Quality Department, Metropolitan Electricity Authority (MEA), Bangkok, Thailand.

REFERENCES

[1] IEEE Standard 1159-1995. 1995. IEEE Recommended Practice for Monitoring Electrical Power Quality.
[2] http://www.ecmweb.com.
[3] Barry, W. Kennedy. 2000. *Power Quality Primer*, McGraw-Hill.
[4] Ford G. L. and Sengupta S. S. 1982. Analytical methods for probabilistic shot circuit studies. *Electric Power Systems Research*, vol 5, pp. 13-20.
[5] Billinton, R., and Allan, R. 1996. *Reliability Evaluation of Power Systems.* Plenum Press: New York.
[6] Math H.J. Bollen. 2000. *Understanding Power Quality Problems : Voltage Sags and Interruptions.* IEEE Press: New York.
[7] Faried, S.O., Billinton,R. and Aboreshaid, S. 2005. Stochastic evaluation of voltage sag and unbalance in transmission system. *IEEE Tran. Power Delivery*, vol. 20, no. 4, pp. 2631-2637.
[8] Bakar, N.A., Mohamed, A., and Ismail, M. 2003. A case study of voltage sag analysis in a utility distribution system. In *Proceedings of Power Engineering Conference*, pp. 333-336.
[9] IEEE Standard 493 – 1997. 1998. IEEE Recommended Practice for the Design of Reliable Industrial and Commercial Power Systems, (Gold Book).
[10] http://www.pscad.com.
[11] Martinez, J.A., and Martin-Arnedo, J. 2004. Voltage sag stochastic prediction using an electromagnetic transients program. *IEEE Trans. Power Delivery*, vol. 19, no. 4, pp. 1975-1982.
[12] Martinez-Velasco, J.A., and Martin-Arnedo, J. 2006. Voltage sag studies in Distribution networks – part II : voltage sag assessment. *IEEE Trans. Power Delivery*, vol. 21, no. 3, pp. 1679-1687.
[13] Martinez-Velasco, J.A., and Martin-Arnedo, J. 2006. Voltage sag studies in Distribution networks – part I : System Modelling. *IEEE Trans. Power Delivery*, vol. 21, no. 3, pp. 1670-1678.
[14] http://www.itic.org.

APPENDIX

Generating Normally Distributed Random Variates

A normally distributed random variate can be generated the normal culmulatime probability distribution function

$F(x)$. The inverse function of $F(x)$ has the following approximate expression [7]:

$$z = t - \frac{\sum_{i=0}^{2} c_i t^i}{1 + \sum_{i=1}^{3} d_i t^i} \quad \text{(A1)}$$

where

$$t = \sqrt{-2 \ln Q} \quad \text{(A2)}$$

$c_0 = 2.515517$ $\quad$ $d_1 = 1.432788$

$c_1 = 0.802853$ $\quad$ $d_2 = 0.189269$

$c_2 = 0.010328$ $\quad$ $d_3 = 0.001308$

The implications of z and Q are shown in Figure A1, where $f(z)$ is the standard normal probability density function.

$$f(z) = \frac{1}{\sqrt{2\pi}} e^{\left[-\frac{z^2}{2}\right]} \quad \text{(A2)}$$

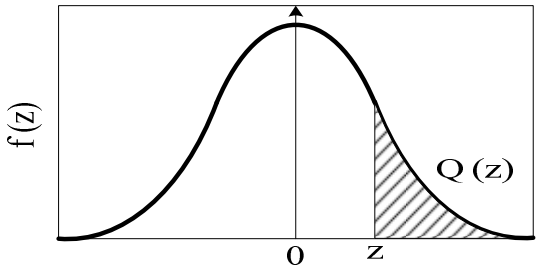

Fig.A1. Area Under Normal Density Function $Q(z)$

Table A1. Load Data of 33-Bus Distribution System

Bus No.	P_L (MW)	Q_L (MVAR)	Bus No.	P_L (MW)	Q_L (MVAR)
3	1.785	0.988	15	1.478	0.818
4	2.783	1.540	16	1.740	0.963
5	2.168	1.200	18	0.420	0.232
6	1.050	0.581	20	0.533	0.295
7	1.628	0.901	21	1.050	0.581
8	1.313	0.726	22	0.656	0.363
10	0.656	0.363	25	1.050	0.581
12	0.822	0.455	26	1.575	0.871
13	0.559	0.309	29	1.313	0.726
14	1.890	1.046	30	2.562	1.418
31	0.525	0.291	33	0.525	0.291
32	0.473	0.261			

Table A2. Equivalent Source Impedance

Source	Impedance (pu.)			
	$R_{1,2}$	$X_{1,2}$	R_0	X_0
PR. Substation Transformer No.3	0.13114	0.42173	0.09547	0.37962

Table A3. Branch Data of 33-Bus Distribution System

From Bus	To Bus	$R_{1,2}$ (pu.)	$X_{1,2}$ (pu.)	R_0 (pu.)	X_0 (pu.)	Length (km)
1	2	0.0233	0.0349	0.1727	0.1754	1.00
1	4	0.0116	0.0174	0.0860	0.0873	0.50
1	9	0.0105	0.0157	0.0778	0.0873	0.45
1	22	0.0022	0.0033	0.0165	0.0873	0.10
2	3	0.0042	0.0062	0.0251	0.0342	0.12
2	31	0.0017	0.0025	0.0101	0.0137	0.05
4	5	0.0069	0.0102	0.0419	0.0570	0.20
5	6	0.1042	0.1537	0.6281	0.8547	3.00
6	7	0.0556	0.0819	0.3350	0.4558	1.60
6	8	0.1250	0.0369	0.0445	0.0730	3.60
9	10	0.0764	0.0225	0.0272	0.0446	2.20
9	13	0.1181	0.0348	0.0420	0.0689	3.40
10	11	0.0972	0.0287	0.0346	0.0568	2.80
11	12	0.1677	0.0492	0.0593	0.0973	4.80
13	14	0.0694	0.0205	0.0247	0.0405	2.00
14	15	0.0972	0.0287	0.0346	0.0568	2.80
15	16	0.1250	0.0369	0.0445	0.0730	3.60
16	17	0.1250	0.0369	0.0445	0.0730	3.60
17	18	0.1250	0.0369	0.0445	0.0730	3.60
17	19	0.1736	0.0512	0.0618	0.1014	5.00
19	20	0.0972	0.0287	0.0346	0.0568	2.80
19	21	0.0972	0.0287	0.0346	0.0568	2.80
22	23	0.0049	0.0014	0.0017	0.0028	0.14
23	24	0.0035	0.0010	0.0012	0.0020	0.10
23	27	0.0174	0.0051	0.0062	0.0101	0.50
24	25	0.0097	0.0029	0.0035	0.0057	0.28
24	26	0.0090	0.0027	0.0032	0.0053	0.26
27	28	0.0028	0.0008	0.0010	0.0016	0.08
28	29	0.0174	0.0051	0.0062	0.0101	0.50
28	30	0.0174	0.0051	0.0062	0.0101	0.50
31	32	0.0035	0.0010	0.0012	0.0020	0.10
32	33	0.0035	0.0010	0.0012	0.0020	0.10

Lightning Performance Improvement of 115 kV and 24 kV Circuits by External Ground in MEA's Distribution System

A. Phayomhom and S. Sirisumrannukul

Abstract*— *This paper presents the guidelines for preparing a paper for GMSARN International Journal. This document can be used as a template if you are using Microsoft Word 6.0 or later. The abstract should contain not more than 200 words. It should outlining the aims, scope and conclusions of the paper. Do not cite references in the abstract. Do not delete the space before Introduction. It sets the footnote.

***Keywords*— About four key words or phrases in alphabetical order, separated by commas.**

1. INTRODUCTION

Metropolitan Electricity Authority (MEA) is responsible for power distribution covering an area of 3,192 square kilometers in Bangkok, Nonthaburi, and Samutprakarn provinces of Thailand. MEA serves approximately 37 % of the whole country power demand. MEA's networks consist of transmissions, subtransmissions, and distribution systems. The voltage level in transmission systems is 230 kV, in subtransmission systems 69 kV and 115 kV, and in distribution systems 12 kV and 24 kV.

Due to the right of way and obstruction in some service areas, a 24 kV circuit have to be installed under a 115 kV circuit on the same concrete pole. In this configuration, the 24 kV and 115 kV circuits share the same lightning protection that uses a ground wire embedded in the pole to provide a grounding path between an overhead ground wire (OHGW) on the top of the pole and a ground rod located in earth under the pole.

The number of thunderstorm days in Bangkok, averaged over the period from 1993 to 1997, is 68 days [1]. Direct or indirect lightning stokes on OHGWs could lead to power interruption as a result of insulation flashover caused by the high energy of the strokes.

When a lightning stroke hits at the OHGW of a 115 kV subtransmission system, an overvoltage is induced on both the phase conductors of the 115 kV and 24 kV systems. This overvoltage can damage insulators by back flashover if the voltage across the insulators exceeds the critical flashover voltage (CFO) of the insulators. This problem can be solved by the method of external ground.

A. Phayomhom (corresponding author) is with the Department of Electrical Engineering, Faculty of Engineering, King Mongkut's University of Technology North Bangkok, Thailand and with Power System Planning Department, Metropolitan Electricity Authority (MEA), 1192 Rama IV Rd., Klong Toey, Bangkok, 10110, Thailand. Phone: +66-2-348-5421; Fax: +66-2-348-5133; E-mail: attp@mea.or.th or att_powermea@yahoo.com.

S. Sirisumrannukul is with the Department of Electrical Engineering, Faculty of Engineering, King Mongkut's University of Technology North Bangkok 1518, Pibulsongkram Rd., Bangsue, Bangkok, 10800, Thailand.

An external ground is attached along the concrete pole connected between the OHGW and a ground rod. It can help reduce the resistance of the ground rod and the surge impedance of the pole. This method gives a reduction in voltage across the insulator units as well as back flashover rate (BFOR). The benefit of an external ground depends on pole span, line configuration, surge impedance of the pole, and resistance of the ground rod.
In this paper, the Alternative Transient Program-Electromagnetic Transient Program (ATP-EMTP) is employed to model and analyze a lightning performance improvement of 115 kV and 24 kV circuits by external grounds. The performances are considered in terms of top pole voltage, critical current and BFOR. Simulation results with and without external grounds for different values of lightning front time and impulse resistance of ground rod are presented.

2. DATA OF SYSTEM STUDIED

Detail of 115 kV and 24 kV circuits

The configuration and grounding system of a 115 kV subtransmission system with underbuilt 24 kV distribution feeders in MEA is shown in Figure 1. The reinforced concrete pole is 20 m high. The 115 kV circuit consists of 2×400 mm^2 all-aluminium conductor (AAC) per phase, while the double circuit of the 24 kV circuit consists of 1×185 mm^2 spaced arial cable (ASC) per phase. A 1×38.32 mm^2 OHGW is directly connected to a ground wire embedded in the concrete pole. The ground wire is connected to a 3-m-long ground rod with a diameter of 15.875 mm [2].

Insulator

A suspension porcelain insulator type 52-3 (see Figure 2) and a pin post porcelain insulator type 56/57-2 (see Figure 3) are commonly seen in MEA's system. The suspension insulator is complied with Thai Industrial Standard: TIS.354-1985 and the pin post insulator with TIS.1251-1994 standard. In a 115 kV subtransmission system, a string of 7 suspension insulator units are installed to support a phase conductor, while in the 24 kV circuit, the pin post insulators support the phase conductor. The critical-impulse flashover values of these two insulators are listed in Table 1 [2].

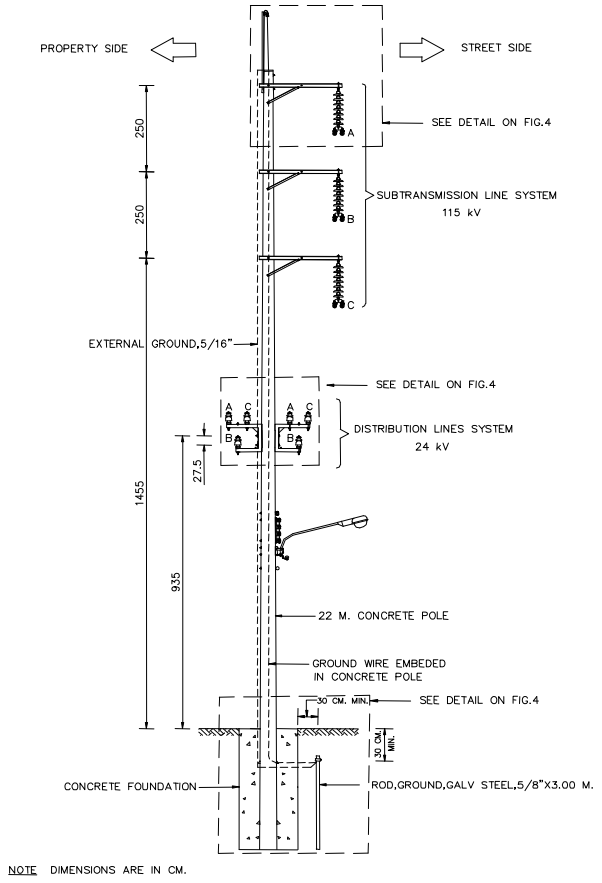

Fig.1. Installation of 115 and 24 kV Circuits in MEA's Network.

Table 1. Critical Flashover Voltage of Insulators [3], [4]

Insulator type	Critical Flashover Voltage	
	Positive (kV)	Negative (kV)
52-3 (7unit)	695	670
56/57-2 (1unit)	180	205

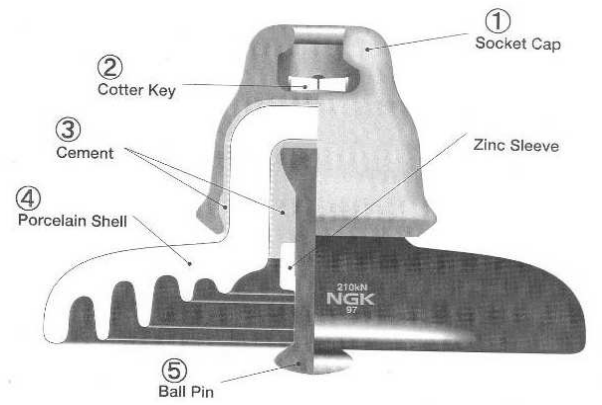

Fig.2. Typical Suspension Insulator Type 52-3.

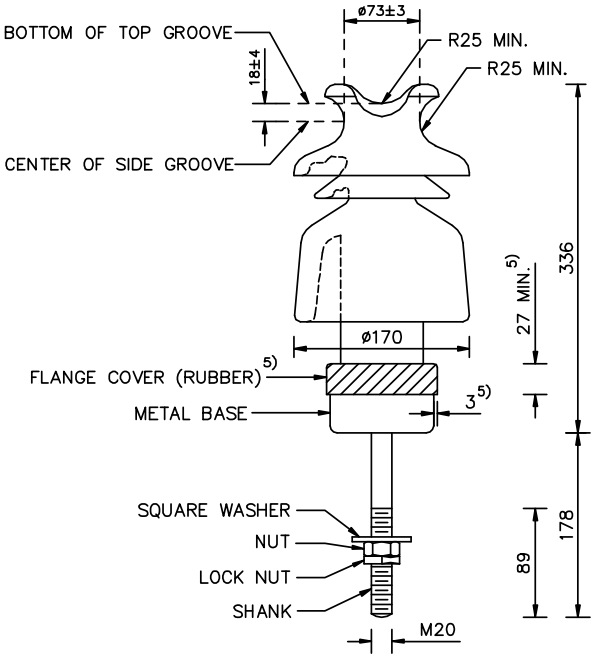

Fig.3. Typical Pin Post Insulator Type 52/57-2.

3. INSTALLATION OF EXTERNAL GROUND

The interruption data in the 115 kV circuits in the year 2006 collected by the Power System Control Department of MEA reveal that lightning strokes resulted in 2 sustained interruptions (interruption duration is greater than or equal to one minute) and 9 momentary interruptions (interruption duration is less than 1 minute). The total length of the 115 kV circuits in MEA's system is 480.30 circuit-kilometers. With these data, the BFOR, calculated from the number of interruptions and the total length, is 2.29 flashes/100 km/year.

In this paper, the method of external ground is applied to the MEA network in order to reduce the back flashover rate (BFOR) value. The method of external ground is implemented by attaching a 1×38.32 mm^2 of zinc-coated steel wire along the concrete pole connected between an overhead ground wire (OHGW) and an existing ground rod. The typical detail of external ground installation and its schematic diagram are provided in Figures 4 and 5.

4. ATP-EMTP MODEL

The proposed ATP-EMTP model used to analyze lightning performance is shown in Figure 6. The 115 kV and 24 kV circuits are represented by AC three-phase voltage sources. The OHGW, subtransmission, and distribution lines are modeled by line constants or cable parameters/cable constants of J.Marti's line model. The ATP-EMTP model is proposed in Figure 6 and needs following parameters:

- Frequency for line modeling
- Lightning current model (Block A)
- Surge impedance of concrete pole (Block B)
- Impulse impedance of the ground rod (Block C)
- Surge impedance of external ground (Block D)

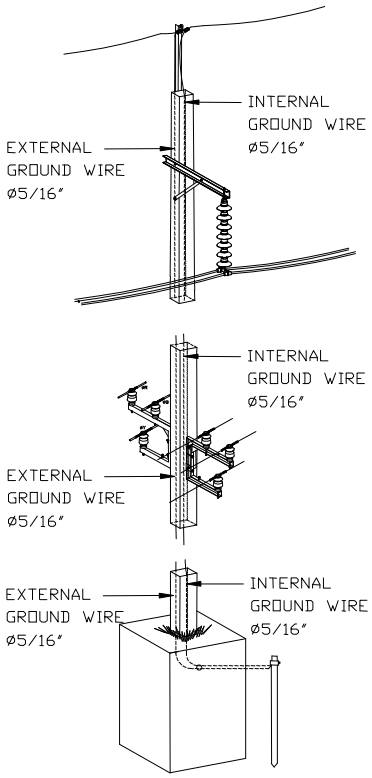

Fig.4. External Ground Installation.

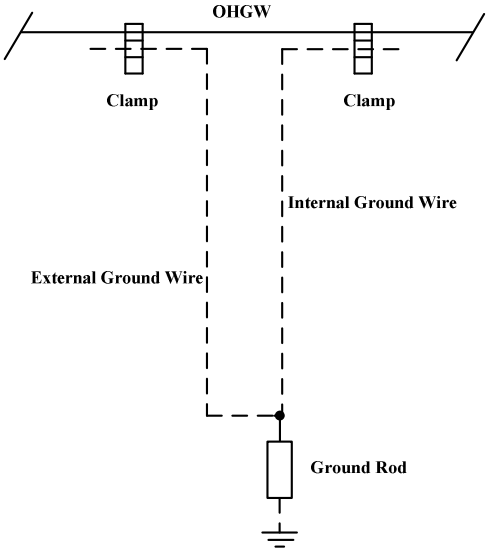

Fig.5. Schematic Diagram of External Ground Installation

Frequency for line modeling

Line parameters (resistance, inductance, and capacitance) are represented by a frequency dependent model of the transient phenomenon of lightning [5]. This frequency varies with the length of line segment. The frequency is calculated by

$$f = \frac{3\times10^{8}}{4l_{line}} \qquad (1)$$

where f = frequency for line modeling (Hz)

l_{line} = line segment of length (m)

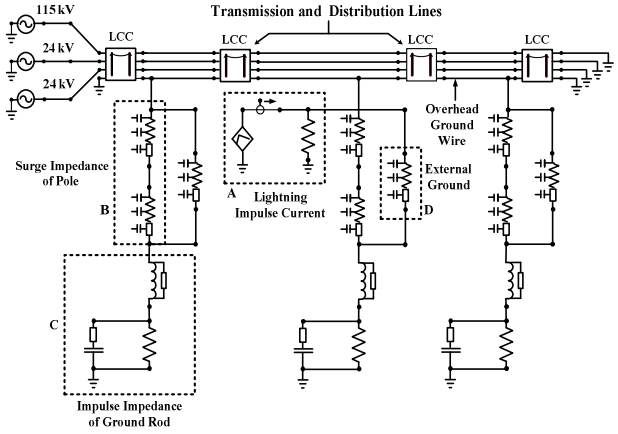

Fig.6. Diagram of ATP-EMTP Model.

Lightning current source model

Lightning is represented by the slope ramp model shown in Figure 7. Three important parameters that identify the characteristic of lightning current waveforms are peak current I_p , front time t_1, and tail time t_2. The peak current is the maximum value of current found in the waveform. The front time is a time interval when the current increases from zero to its peak. The tail time is the sum of the front time and the time that the current falls to 50% of its peak value.

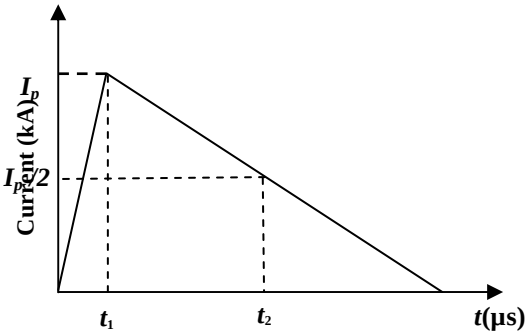

Fig. 7. Lightning Current Waveform.

Surge impedance of pole

Surge impedance of pole (Z_T) is the impedance of the grounding path. Its value depends on the height of the pole and the size of the ground wire. Z_T can be expressed as [6]:

$$Z_T = 60\ln\left(\frac{H}{r}\right) + 90\left(\frac{r}{H}\right) - 60 \qquad (2)$$

where Z_T = surge impedance pole (Ω)
H = pole height (m)
γ = radius of ground wire (m)

Impulse impedance of the ground rod

An equivalent circuit of the ground rod is shown in Figure 8. The resistance, inductance, and capacitance of the under transient phenomenon are calculated by [7], [8]:

$$R_i = \alpha R_0 \tag{3}$$

$$R_0 = \frac{\rho}{2\pi l}\left(\ln\frac{8l}{d} - 1\right) \tag{4}$$

$$L = 2l\left(\ln\frac{4l}{d}\times 10^{-7}\right) \tag{5}$$

$$C = \frac{\varepsilon_r l}{18\ln\left(\frac{4l}{d}\right)}\times 10^{-9} \tag{6}$$

where R_i = impulse resistance of ground rod (Ω)
α = impulse coefficient
R_0 = resistance of ground rod at power frequency (Ω)
ρ = soild resistivity (Ω-m)
l = total length of ground rod (m)
d = diameter of ground rod (m)
L = inductance of ground rod (H)
C = capacitance of ground rod (F)
ε_r = relative permittivity of solid

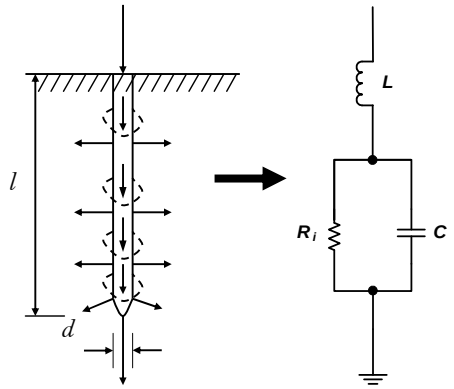

Fig.8. Equivalent Circuit for Ground Rod under Impulse Condition.

Surge impedance of external ground

A good approximation for the surge impedance of an external ground is given in (7) [9], whose parameters are based on those of the MEA standard as presented in Table 2.

Table 2. Parameters in ATP-EMTP Modeling

Detail	Values	Model
1. Lightning current		
- Amplitude (kA)	34.4	Ramp
- Front time/tail time (μs) [10],[11]	0.25/100, 10/350	
2. OHGW		
- Diameter (mm)	7.94	
- DC resistance (Ω)	3.60	
3. Phase conductor of 115 kV		
- Diameter (mm)	25.65	J.Marti
- DC resistance (Ω)	0.0778	
4. Phase conductor of 24 kV		
- Diameter (mm)	15.35	
- DC resistance (Ω)	0.164	
5. Pole		
- Height (m)	20	
- Span (m)	80	
- Surge impedance (Ω)	451.4	
- Wave velocity (m/μs) [12]	123	
6. External ground		
- Diameter (mm)		Distributed Parameter
- Length (m)	20	
- Surge impedance (Ω)	411.27	
- Wave velocity (m/μs) [12]	300	
7. Ground rod		
- Diameter (mm)	16	
- Length (m)	3	
- Impulse resistance (Ω)	5-100	

$$Z_{gc} = 60\ln\left(\frac{h}{er}\right) - k\ln\left(1+\left(\frac{r_c}{D}\right)\right) \tag{7}$$

$$k = 0.096\times r_c + 13.95 \tag{8}$$

where Z_{gc} = surge impedance external ground (Ω)
h = conductor height (mm)
r = conductor radius (mm)
e = base of natural logarithm
k = constant
r_c = radius of pole (mm)
D = separate distance between skill of reinforced concrete pole and grounding conductor (mm)

5. LIGHTNING PERFORMANCE INDICES

Three lightning performance indices are considered: 1) top pole voltage, 2) critical current and 3) BFOR. The top pole voltage in a 115 kV circuit is a voltage-to-ground of the OHGW. For the underbuilt 24 kV circuit, the top pole voltage is a voltage-to-ground of the bonding point connected to the grounding system of the 115 kV. The critical current is defined as lightning stroke current when injected into the conductor causing flashover. When the critical current is known, BFOR, expressed in flashovers per length of line per year, can be calculated by: [1], [13], [14].

$$BFOR = P(I) \times N_l \tag{9}$$

$$P(I) = \frac{1}{\left(1+\left(\frac{I}{A}\right)^B\right)} \tag{10}$$

$$N_l = N_g\left(\frac{28h^{0.6}+b}{10}\right) \tag{11}$$

$$Ng = 0.0133T_d^{1.25} \tag{12}$$

where

$BFOR$ = back flashover rate (flashes/100 km/yr)
$P(I)$ = probability distribution of stroke current peak magnitude
I = first stroke peak current magnitude (kA)
A = median of stroke peak current magnitude (kA)
B = constant (2.6 for Thailand power system) [1]
N_l = number of lightning strikes (flashes/100 km/yr)
N_g = ground flash density (flashes/km^2/yr)
h = average conductor height (m)
b = separation distance of overhead ground wire (m)
T_d = number of thunderstorms (days/yr)

6. CASE STUDY

The system in Figure 1 is simulated by the ATP-EMTP program. The lightning performance of this system is analyzed by two lightning current waveforms, 0.25/100 µs and 10/350 µs, with and without an external ground for different impulse resistances of the ground rod. The test results are derived from a lightning current magnitude of 34.4 kA, which is the median of stroke peak current magnitude over the period from 1993 to 1997 in Thailand [1]. Simulation results are shown in Tables 3-8.

The numerical results under the 0.25/100 µs waveform in Tables 3 reveal that without an external ground in the 115 kV circuit, the top pole voltage remains unchanged for different impulse resistances. The reason is that the top pole voltage cannot be attenuated by the reflected wave generated by the impulse resistance of the ground rod. But this is not the case for the 10/350 µs waveform (Table 4) because its font time is 40 times longer than that of the other and for the 24 kV circuit because the reflected wave travels shorter to the bonding point.

An external ground helps reduce the top pole voltage particularly for the 0.25/100 µs waveform since the reflected wave can travel through the grounding path faster and therefore reducing the top pole voltage. However, for the 10/350 µs waveform if the impulse resistance is greater than 50 Ω for 115 kV and 10 Ω for 24 kV, the top pole voltage will stay constant owning to reduction in the reflected coefficient magnitude.

Table 3. Top Pole Voltage for 0.25/ 100 µs Waveform (kV)

R_i (Ω)	115 kV		24 kV	
	External ground		External ground	
	without	with	without	with
5	5,678.60	3,368.20	4,010.20	2,844.40
10	5,678.60	3,385.40	4,042.20	2,872.50
25	5,678.60	3,430.20	4,138.70	2,945.90
50	5,678.60	3,488.50	4,256.80	3,099.20
75	5,678.60	3,532.60	4,339.80	3,340.10
100	5,678.60	3,566.80	4,421.90	3,531.70

Table 4. Top Pole Voltage for 10/ 350 µs Waveform (kV)

R_i (Ω)	115 kV		24 kV	
	External ground		External ground	
	without	with	without	with
5	250.63	161.24	167.70	140.97
10	276.01	225.18	214.39	214.39
25	363.75	359.94	335.55	335.55
50	457.33	457.33	447.42	447.42
75	504.67	504.67	499.70	499.70
100	528.07	528.07	525.58	525.58

Table 5 shows that with an external ground, the system is able to withstand more critical current, for example under the 0.25/ 100 µs waveform, as much as 56% - 70% for 115 kV and 20% - 40% for 24 kV. But under the 10/350 µs waveform in Table 6, the increase of critical current becomes less obvious when the impulse resistance is increased for the same reason used to explain the top pole voltage of Table 4.

The mathematical relation between critical current and BFOR, as expressed in (9) and (10), indicates that increasing the critical current decreases $P(I)$ and hence BFOR. It is shown from Tables 7 and 8 that BFORs under the 0.25/100 µs waveform for both 115 kV and 24 kV circuits are slightly different. An external ground does not much affect BFOR in the 115 kV and 24 kV

circuits. With the 10/350 µs waveform, the maximum reductions of BFOR in both circuits are only achieved by the 5 Ω impulse resistance.

Table 5. Critical Current for 0.25/ 100 µs Waveform (kA)

R_i (Ω)	115 kV		24 kV	
	External ground		External ground	
	without	with	without	With
5	4.60	7.80	2.00	2.80
10	4.60	7.60	1.98	2.70
25	4.60	7.60	1.95	2.70
50	4.60	7.40	1.85	2.50
75	4.60	7.30	1.83	2.30
100	4.60	7.20	1.80	2.15

Table 6. Critical Current for 10/350 µs Waveform (kA)

R_i (Ω)	115 kV		24 kV	
	External ground		External ground	
	without	with	without	with
5	103.30	170.00	54.00	60.00
10	100.00	120.00	40.00	40.00
25	74.00	75.00	24.50	24.50
50	60.00	60.00	18.00	18.00
75	55.00	55.00	15.00	15.00
100	53.00	53.00	14.00	14.00

Table 7. BFOR for 0.25/100 µs Waveform (flashes/100 km/yr)

R_i (Ω)	115 kV		24 kV	
	External ground		External ground	
	without	with	without	with
5	43.59	42.83	43.80	43.80
10	43.59	42.90	43.80	43.80
25	43.59	42.90	43.80	43.80
50	43.59	42.96	43.82	43.82
75	43.59	42.99	43.83	43.83
100	43.59	43.02	43.84	43.84

As seen in Tables 7 and 8, the 5 Ω of impulse resistance (R_i) is optimal for the installation of external ground. Thereby, the economic analysis of external ground is performed only in this value of R_i. The net present value (NPV), which is defined as the total present value (PV) of a time series of cash flows [15], is applied to demonstrate the economic merit.

The breakdown of investment cost for the installation of external ground depicted in Figure 4 is listed in Table 9. From this table, the total investment cost for 100 km subtransmission lines can be calculated as 502,038.81 Baht. It was reported in [16] that the interruption cost per event in MEA's service area was 147,500 Baht/event in the year 2000. The total investment cost and the interruption cost are respectively equivalent to 712,037.08 Baht/100 km and 258,016 Baht/event with a discount rate of 7.24%. The total outage cost can be estimated by the product of 258,016 Baht/event and BFOR. The total investment cost and total outage cost are then used in the calculation of NPV with the same discount rate (7.24 %) over a period of 25 years. The NPV in case of with and without external ground are shown in Tables 10 and 11. Note that the cash flows for the investment cost are considered as positive. The total NPV for each lightning waveform is the summation of NVP from 115 kV and 24 kV circuits whereas the total expected NPV is calculated by assuming that both waveforms are equally likely to occur (i.e., 50% chance). The lower expected value in case of the system with external ground indicates the economic merit to implement this proposed technique to MEA'system.

Table 8. BFOR for 10/350 µs Waveform (flashes/100 km/yr)

R_i (Ω)	115 kV		24 kV	
	External ground		External ground	
	without	with	without	with
5	2.64	0.79	10.74	8.47
10	2.85	1.85	17.85	17.85
25	5.63	5.47	30.73	30.73
50	8.74	8.74	36.63	36.63
75	10.37	10.37	38.98	38.98
100	11.12	11.12	39.69	39.69

Table 9. Breakdown of Investment Cost (Baht/pole)

Item	Investment Cost (Baht/pole)
Material	425.65
Labor	54.25
Work Control	16.28
Transportation	21.28
Operation	25.87
Miscellaneous	25.87
Total	569.20

Table 10. Net Present Value with External Ground (Million Baht/100 km)

Description	Waveform	
	0.25/100 (µs)	10/350 (µs)
NPV of 115 kV Circuit	126.29	3.28
NPV of 24 kV Circuit	129.85	3.28
Total Circuit	256.14	6.56
Total expected NPV	131.35	

Table 11. Net Present Value without External Ground (Million Baht/100 km)

Description	Waveform	
	0.25/100 (μs)	10/350 (μs)
NPV of 115 kV Circuit	128.28	7.77
NPV of 24 kV Circuit	128.90	7.77
Total Circuit	257.18	15.54
Total expected NPV	136.36	

From the economic and reliability advantages of external ground installation, this proposed technique can be served as a guideline to develop the performance of MEA's distribution system because this proposed technique can increase the reliability of system and is able to reduce the electricity failure due to back flashover.

7. CONCLUSION

This paper has presented the lightning performance improvement of 115 and 24 kV circuits installed on the same pole by an external ground in MEA's distribution network. The lightning performance is evaluated by 0.25/100 μs and 10/350 μs lightning current waveforms and different impulse resistances. The test results obtained from the ATP-EMTP indicate that top pole voltage, critical current, and BFOR can be improved when an external ground is installed. The advantages of external ground depend on lightning current waveform and impulse resistance of ground rod. In addition, the test results also reveal that low impulse impedance is suitable for external ground.

ACKNOWLEDGMENT

The first author would like to express his sincere thanks to Metropolitan Electricity Authority (MEA), Thailand for the technical data used in this research work.

REFERENCES

[1] Wattanasakpubal, C. 2003. Improve lightning performance 115 kV transmission line's PEA by external ground. Master thesis King Mongkut's University of Technology North Bangkok. Thailand. (in Thai).

[2] Power System Planning Department, Metropolitan Electricity Authority. 2000. MEA Overhead Subtransmisson Construction Standard. DWG. No. 10A4-0524.

[3] TIS.354-1985. 1985. Suspension Insulator Type 52-3. Bangkok: Thai Industrial Standards Institute.

[4] TIS.1251-1994. 1994. Pin Post Insulator Type 56/57-2. Bangkok: Thai Industrial Standards Institute.

[5] Alberto, R., et al. 2001. Non uniform line tower model for lightning transient studies. In *Proceedings of Power System Transients*, Rio de Janeiro, Brazil, 24-28 June.

[6] Zhijing, Z., et al. 2004. The Simulation model for calculating the surge impedance of a tower. In *Proceedings of IEEE International Symposium on Electrical Insulation*, Indianapolis, USA,19-22 September.

[7] Jinliang, H., et al. 1998. Impulse characteristics of grounding systems of transmission-line towers in the regions with high soil resistivity. In *Proceedings of Power System Technology*, Beijing, China, 18-21 August.

[8] El-Morshedy, A. et al. 2000. *High-Voltage Engineering*. New York: Marcel Dekker & Co (Pubishers) Ltd.

[9] Mozumi, T., et al. 2001. An empirical formula for the surge impedance of a grounding conductor along a reinforced concrete pole in a distribution line. In *Proceedings of* Power System Transients Rio de Janeiro, Brazil, June 24-28.

[10] IEC 61024-1. 1990. Protection of structures against lightning Part 1: General principles.

[11] IEC 61312-1. 1995. Protection against lightning electromagnetic Part 1: General principles.

[12] Hintamai, S., and Hokierti, J. 2006. Analysis of electrical reinforced concrete pole grounding effects to overvoltage in high voltage. In *Proceedings of 29th Electrical Engineering Conference*. Thailand, 9-10 November. (in Thai)

[13] IEEE Std 1243-1997. Guide for Improving the Lightning Performance of Transmission Lines.

[14] Whitehead, J.T., and et al. Estimation Lightning Performance of Transmission Lines II – Updates to Analytical Models. *IEEE Working Group Report, IEEE Trans. Power Delivery*, 8(3): July, 1254-1267.

[15] Grant, E. L. and Ireson, W. G. and Leavenworth,R. S. 1990. *Principles of Engineering Economy*. John Wiley & Sons.

[16] Energy Research Institute Chulalongkorn University. 2001. *Electricity Outage Cost Study*. Bangkok: Chulalongkorn University.

GMSARN International Journal
NOTES FOR AUTHORS

Editorial Policy

In the Greater Mekong Subregion, home to about 250 million people, environmental degradation - including the decline of natural resources and ecosystems will definitely impact on the marginalized groups in society - the poor, the border communities especially women and children and indigenous peoples. The complexity of the challenges are revealed in the current trends in land and forest degradation and desertification, the numerous demands made on the Mekong river - to provide water for industrial and agricultural development, to sustain subsistence fishing, for transport, to maintain delicate ecological and hydrological balance, etc., the widespread loss of biological diversity due to economic activities, climate change and its impacts on the agricultural and river basin systems, and other forms of crises owning to conflicts over access to shared resources. The *GMSARN International Journal* is dedicated to advance knowledge in energy, environment, natural resource management and economical development by the vigorous examination and analysis of theories and good practices, and to encourage innovations needed to establish a successful approach to solve an identified problem.

The *GMSARN International Journal* is a biannual journal published by GMSARN in June and December of each year. Papers related to energy, environment, natural resource management, and economical development are published. The papers are reviewed by world renowned referees.

Preparation Guidelines

1. The manuscript should be written in English and the desired of contents is: Title, Author's name, affiliation, and address; Abstract, complete in itself and not exceeding 200 words; Text, divided into sections, each with a separate heading; Acknowledgments; References; and Appendices. The standard International System of Units (SI) should be used.

2. Illustrations (i.e., graphs, charts, drawings, sketches, and diagrams) should be submitted on separate sheets ready for direct reproduction. All illustrations should be numbered consecutively and given proper legends. A list of illustrations should be included in the manuscript. The font of the captions, legends, and other text in the illustrations should be Times New Roman. Legends should use capital letters for the first letter of the first word only and use lower case for the rest of the words. All symbols must be italicized, e.g., α, θ, Q_{wt}. Photographs should be black and white glossy prints; but good color photographs are acceptable.

3. Each reference should be numbered sequentially and these numbers should appear in square brackets in the text, e.g. [1], [2, 3], [4]–[6]. All publications cited in the text should be presented in a list of full references in the Reference section as they appear in the text (not in alphabetical order). Typical examples of references are as follows:

   - **Book references** should contain: name of author(s); year of publication; title; edition; location and publisher. Typical example: [2] Baker, P.R. 1978. Biogas for Cooking Stoves. London: Chapman and Hall.
   - **Journal references** should contains: name of author(s); year of publication; article title; journal name; volume; issue number; and page numbers. For example: Mayer, B.A.; Mitchell, J.W.; and El-Wakil, M.M. 1982. Convective heat transfer in veetrough liner concentrators. Solar Energy 28 (1): 33-40.
   - **Proceedings reference** example: [3] Mayer, A. and Biscaglia, S. 1989. Modelling and analysis of lead acid battery operation. Proceedings of the Ninth EC PV Solar Conference. Reiburg, Germany, 25-29 September. London: Kluwer Academic Publishers.
   - **Technical paper** reference example: [4] Mead, J.V. 1992. Looking at old photographs: Investigating the teacher tales that novice teachers bring with them. Report No. NCRTL-RR-92-4. East Lansing, MI: National Center for Research on Teacher Learning. (ERIC Document Reproduction Service No. ED346082).
   - **Online journal** reference example: [5] Tung, F. Y.-T., and Bowen, S. W. 1998. Targeted inhibition of hepatitis B virus gene expression: A gene therapy approach. Frontiers in Bioscience [On-line serial], 3. Retrieved February 14, 2005 from http://www.bioscience.org/1998/v3/a/tung/a11-15.htm.

4. Manuscript can be uploaded to the website or sent by email. In case of hard copy, three copies of the manuscript should be initially submitted for review. The results of the review along with the referees' comments will be sent to the corresponding author in due course. At the time of final submission, one copy of the manuscript and illustrations (original) should be submitted with the diskette. Please look at the author guide for detail.

GMSARN Members

Asian Institute of Technology

Hanoi University of Technology

Ho Chi Minh City University of Technology

Institute of Technology of Cambodia

Khon Kaen University

Kunming University of Science and Technology

National University of Laos

Royal University of Phnom Penh

Thammasat University

Yangon Technological University

Yunnan University

Guangxi University

Associate Members

Nakhon Phanom University

Mekong River Commission

Ubon Rajathanee University

Published by the **Greater Mekong Subregion Academic and Research Network (GMSARN)**
c/o Asian Institute of Technology (AIT)
P.O. Box 4, Klong Luang
Pathumthani 12120, Thailand
Tel: (66-2) 524-5437; Fax: (66-2) 524-6589
E-mail: gmsarn@ait.ac.th
Website: http://www.gmsarn.org